FOSSIL

DR#0656-4

DOE/PC/80519-T1
(DE89005257)

DIFFUSION OF GASES IN COALS AND CHARS

Final Report for the Period of Performance September 15, 1985—September 14, 1988

By
Douglas M. Smith

Work Performed Under Contract No. FG22-85PC80519

For
U. S. Department of Energy
Pittsburgh Energy Technology Center
Pittsburgh, Pennsylvania

By
University of New Mexico
Albuquerque, New Mexico

DISCLAIMER

DISCLAIMER

Price: Printed Copy A04
Microfiche A01

Printed in the United States of America, Office of Scientific and Technical Information, Oak Ridge , Tennessee

DOE/PC/80519-T1
(DE89005257)
Distribution Category UC-102

DIFFUSION OF GASES IN COALS AND CHARS

FINAL REPORT

PERIOD OF PERFORMANCE
9/15/85-9/14/88

DOE/PC80519

By

Douglas M. Smith
UNM POWDERS AND GRANULAR MATERIALS LABORATORY
Department of Chemical and Nuclear Engineering
University of New Mexico
Albuquerque, NM 87131
(505)-277-2861

THIS PAGE

WAS INTENTIONALLY

LEFT BLANK

ABSTRACT

Eight PSOC coals representing a wide range of rank and geographic origin have been subjected to a wide range of pore structure analysis methods as well as gas diffusion measurements. Pore structure analysis techniques employed included carbon dioxide and nitrogen adsorption, helium pycnometry, mercury porosimetry, and low-field NMR spin-lattice relaxation measurements.

In principle, NMR pore structure analysis avoids many of the problems associated with conventional pore structure methods such as pore structure changes during drying, sample compression, network/percolation effects, pore shape assumptions, and a limited pore size range. Spin-lattice relaxation measurements were conducted at a proton frequency of 20 MHz and 303 K using water contained in the coal pores. Pore size distributions were obtained via deconvolution of the NMR relaxation measurements using the method of regularization and application of the "two fraction-fast exchange" model of pore fluid behavior. A qualitative comparison of the NMR pore size distributions and surface areas (CO_2/N_2) yielded good agreement. Monodisperse and bidisperse pore size distributions were noted with pore volume in the size range of <0.5 nm to 0.5 μm.

Effective diffusivities of methane and nitrogen were measured at 303 K and ambient pressure using a pulse tracer analysis method. The measured effective diffusivities ranged from 1.82×10^{-7} to 1.11×10^{-4} cm^2/s for nitrogen and 2.93×10^{-7} to 3.70×10^{-5} cm^2/s for methane. The diffusivity was a strong function of particle size indicating that the unipore diffusion model was not appropriate. Plots of inverse diffusivity inverse particle size squared were linear which allowed extraction of micropore diffusion parameters.

1. INTRODUCTION

The basic philosophy of the investigation was to perform gas-phase diffusion measurements and a wide range of pore structure analysis schemes to the same suite of coal samples. Pore structure analysis included conventional approaches such as gas adsorption and mercury porosimetry as well as a new technique which uses low-field spin-lattice relaxation measurements(developed as part of this project).

2. RESULTS AND DISCUSSION

2.1 DIFFUSION STUDIES

INTRODUCTION

Effective diffusivity measurements for coal are important in a number of applications. For example, the study of methane diffusion through coal is of interest for the production of natural gas from coal beds. It has been assumed [1] that the rate of methane released from a single coal particle is controlled by the diffusion of methane through the pore structure of the coal, since methane is physically adsorbed on the solid surface. In the combustion of coal, the rate of reaction may be controlled by the rate of diffusion of gaseous reactants to the internal pore structure of the coal [2].

Despite the practical necessity for information about gas diffusion through coal, little work has been done to establish diffusion coefficients of gases in coal. Studies to date have been of three different types. The first type consists of flowing a gas through a solid coal disk and, from the measured pressure drop and flow rate, a diffusion coefficient may be calculated. In the second technique, after undergoing a step-change in surface concentration, the rate of adsorption (or desorption) from small

particles is used to determine a diffusion coefficient. The third technique, and the one employed for this study, uses the gas solid chromatography method to measure diffusion parameters for gases in coal. In past diffusion studies, the pore structure of the samples was not studied. In this work, we will study coals with well-characterized pore structure in an effort to relate pore structure and diffusion rates.

BACKGROUND

There are two studies that utilize the flow-disk experiment to study diffusion of gases in coal. Thimons and Kissell [3] used this technique to study methane and helium diffusion in three eastern United States coals. Experiments were undertaken at pressures ranging from 69 to 275 kPa and ambient temperature. Surface transport of adsorbed methane was negligible as compared to gas phase transport and steady-state diffusion coefficients (D_e) were on the order of 10^{-4} to 10^{-5} cm^2/s and the transient D_e's were 0.5 to 10 times the steady-state values. Also, the ratio of $(N_{He}/ N_{CH_4})^{1/2}$, where N_x is the flux of the diffusing gas, was much greater than 2, indicating a strong molecular sieve effect. When the coal was saturated with water vapor, D_e decreased by a factor of 3 to 75. Although Thimons and Kissell addressed several important points, they avoided the question of pore size and size distribution effects by using the unipore model. This model assumes that all pores are of the same diameter and are cylindrical. Other studies [4,5] have indicated that this model fails with coal.

Sevenster [2] used the flow-disk experiment to study a wide variety of gases diffusing through a single British coal using the unipore model. In contrast to the Thimons and Kissell [3] work, the fraction of each species transported by surface diffusion was significant except for He, H_2, N_2, and CO. In the same study, Sevenster utilized the particle adsorption technique

to measure transient D_e in three different coals. Sevenster measured the volumetric uptake of oxygen and water vapor by coal particles (60 mesh-Tyler). Assuming a unipore model, by plotting the fractional uptake, V_t/V_∞, against $t^{1/2}$, D_e can be calculated from the slope of the straight line which should result in the initial uptake region. For oxygen adsorption, straight line (V_t/V_∞ versus $t^{1/2}$) behavior was seen in the 40 to 100 percent V_t/V_∞ region indicating that the unipore model was invalid. Diffusion coefficients for oxygen (303 K and 670 mm Hg) were on the order of 4.5×10^{-14} cm^2/s and appeared to be independent of pressure. The adsorption of water was rapid with 70 percent of the equilibrium amount being adsorbed during the first 100 minutes, after which adsorption was slow, with equilibrium being reached after 24 hours. It should be noted that none of the experimental lines on the V_t/V_∞ versus $t^{1/2}$ plots passed through the origin. Diffusion coefficients for water vapor (298 K and 21 mm Hg) were on the order of 4.8×10^{-13} cm^2/s and there was an increase in D_e with an increase in pressure.

There is a large discrepancy between the diffusion coefficients obtained via the steady state flow experiment and those obtained by the transient adsorption experiment. For oxygen, D_e from the flow experiment was 1.14×10^{-11} cm^2/s and from the adsorption experiment it was 4.5×10^{-14} cm^2/s. For water vapor, D_e was 1.24×10^{-11} cm^2/s from the flow experiment and it was 4.8×10^{-13} cm^2/s from the adsorption experiment. This discrepancy may be attributed to the use of only one small particle size because later studies [4] have shown that D_e's obtained by adsorption experiments are dependent on particle size. This problem is related to the question of the correct characteristic diffusion length.

Nandi and Walker [6] utilized the particle desorption technique to measure D_e in four coals. They were concerned with explaining the large

deviation between surface areas measured with N_2 and CO_2. The study was limited to small particle sizes (-200/+325 Tyler Mesh) and measurements were conducted over a temperature range of 298 to 413 K. The diffusion process was found to be activated and the CO_2 activation energy was significantly lower than that for N_2. Nandi and Walker [7] also studied the diffusion of methane in American coals of rank varying from low volatile matter anthracite to high volatile content bituminous. Diffusion in the micropores was found to be activated, with the activation energy varying from 3.5 kcal/mol for the anthracite to 7.0 kcal/mol for bituminous coals. This suggested that the average size of the accessible micropores in the anthracites is larger than that in the bituminous coals.

One of the most significant differences in that investigation compared to previously discussed studies was in defining two different characteristic diffusion lengths. To obtain D_e, the correct length must be known. The first characteristic length was defined as the ratio of the specific volume, found by He penetration, to the N_2 surface area. The second characteristic length was the ratio of specific volume found using He to neopentane surface area. D_e values for the different coals ranged from 0 x 10^{-16} cm^2/s to 2.4 x 10^{-13} cm^2/s (203-811 kPa and 345 K). In contrast, most investigators employ the particle radius as the characteristic length and obtain much larger D_e values. The correct characteristic length should result in the same diffusivity values for any particle size.

Airey [4] studied methane desorption from an English coal and concluded that the unipore model was inadequate to describe diffusion over the entire timescale and employed an empirical equation of the form:

$$V_t / V_\infty = 1 - e^{-(t/T_o)^n} \qquad (1)$$

Airey found that the moisture content (5.0-6.2 $^{a}H_2O$) of the coal had no effect on the desorption rate, that the quantity of methane adsorbed was independent of particle size but was a strong function of moisture content, that the value of n was independent of particle size and moisture content, and that the value of T_o increased linearly with particle size.

Smith and Williams [5] studied methane desorption from a sub-bituminous coal. Effective diffusivities ranged from 7.93×10^{-6} cm^2/s to 2.26×10^{-5} cm^2/s for six samples from widely different parts of the same formation. Their main objective was to determine if the effective diffusivities calculated from data at short times would correlate over the entire timescale of desorption. They concluded that experimental data agreed well for $V_t/V_\infty < 0.5$ but there was significant deviation between the unipore model and experimental values of V_t/ V_∞ at large times. Since many coals exhibit bidisperse pore size distributions [8], Smith and Williams present a bidisperse pore model for coal which accurately described methane desorption rates over the entire time scale of desorption. The bidisperse pore model required three parameters to describe diffusion through the pores. These parameters are micropore effective diffusivity, macropore effective diffusivity, and a constant which is proportional to the micropore/macropore distribution of gas at equilibrium. In another work, Smith and Williams [9] implemented this bidisperse pore model and used the gas solid chromatography technique coupled with frequency analysis to determine these diffusion parameters.

Many of the discrepancies between the various diffusion studies can be attributed to pore structure variation and different diffusion lengths. It is widely recognized that coal contains pores over a wide range of pore sizes [8,10]. Gan, Nandi and Walker [8] studied the pore structure of a number of coals varying in rank from anthracite to lignite using gas

adsorption, helium and mercury displacement, and mercury porosimetry. Many coals had a bidisperse pore structure with significant fraction of the pore volume being found in the macro and micro pore ranges. Gallegos, Smith and Stermer [10] studied the pore structure of 19 coals using adsorption, mercury porosimetry, helium displacement and nuclear magnetic resonance (NMR) spin-lattice relaxation measurements. CO_2 adsorption at 273 K was used to find the total surface area and N_2 adsorption at 77 K was used to determine surface area in the pore range of $r_p > 1$ nm. Similar to Gan, Nandi and Walker [8], no relationship between carbon content and either the N_2 or CO_2 surface area was found for the 19 different coals. Also, no correlation between carbon content and N_2 pore volume (1 nm < r_p < 33 nm) was found. Porosimetry results were complicated by inter-particle filling, surface roughness and sample compression. Glaves and co-workers [11] have studied many of these same coals using spin-lattice relaxation measurements of water contained in saturated coal samples in order to extract pore size distributions. Qualitative agreement between the NMR measurements and gas adsorption/condensation results was obtained.

EXPERIMENTAL

For porous solids, Schneider and Smith [12] have used gas solid chromatography to determine adsorption equilibrium constants (K_A), adsorption rate constants (k_{ads}), axial dispersion coefficients (D_L), and unipore effective diffusivities. By combining a mass balance of the tracer in the gas phase, a mass balance of this component in the particle, and assuming a linear adsorption isotherm, the concentration of the adsorbing gas as a function of time and axial position, c(z,t), in the packed bed can be obtained:

$$D_L(\partial^2 c/\partial z^2) - u(\partial c/\partial z) - \partial c/\partial t - (3D_e/R)[(1-\alpha)/\alpha](\partial c_i/\partial r)_{r=R} = 0 \quad (2)$$

$$(D_e/\theta)[\partial^2 c_i/\partial r^2 + (2/r)\partial c_i/\partial r] - \partial c_i/\partial t - (\rho_p/\theta)\partial c_{ads}/\partial t = 0 \quad (3)$$

$$\partial c_{ads}/\partial t = k_{ads}(c_i - c_{ads}/K_A) \quad (4)$$

Boundary and initial conditions are:

$$D_e(\partial c_i/\partial r)_{r=R} = k_f(c - c_i) \quad (5)$$

$$\partial c_i/\partial r = 0 \quad \text{at } r=0 \quad \text{for } t > 0 \quad (6)$$

$$c = c_o \quad \text{at } z = 0 \quad \text{for } 0 \leq t \leq t_o \quad (7)$$

$$c = 0 \quad \text{at } z = 0 \quad \text{for } t > t_o \quad (8)$$

where k_f is the external mass transfer coefficient and t_o is the tracer pulse time. By using a Laplace-Carson transform, it is possible to obtain expressions for the moments of the elution curve. The first absolute moment, μ_1', and the second central moment, μ_2, are defined as:

$$A = \int_0^\infty c(z,t)\, dt \quad (9)$$

$$\mu_1' = (1/A)\int_0^\infty c(z,t)\, t\, dt \quad (10)$$

$$\mu_2 = (1/A)\int_0^\infty (t-\mu_1')^2 c(z,t)\, dt \quad (11)$$

The first moment characterizes the position of the curve's center of gravity, whereas the second central moment depends on the width of the curve. These moments are related to the desired transport parameters by [12]:

$$\mu_1' = (z/u)(1+\delta_o) + t_o/2 \quad (12)$$

$$\mu_2 = 2(z/u)[\delta_1 + D_L(1+\delta_o)^2(1/u^2)] - t_o^2/12 \quad (13)$$

$$\delta_o = [(1-\alpha)\theta/\alpha][1 + (\rho_p/\theta)K_A] \quad (14)$$

$$\delta_1 = \delta_a + \delta_i + \delta_e \quad (15)$$

$$\delta_a = [(1-\alpha)/\alpha]\theta(\rho_p/\theta)(K_A^2/k_{ads}) \quad (16)$$

$$\delta_i = (\delta_o R^2\theta/15)[1 + (\rho_p/\theta)K_A](1/D_e) \quad (17)$$

$$\delta_e = (\delta_o R^2\theta/15)[1 + (\rho_p/\theta)K_A](5/k_f R) \quad (18)$$

Where u is the linear velocity of the carrier gas and the parameters which characterize the column and the adsorbent are defined as follows: column length (z), void fraction of the bed (α), porosity of the adsorbent (θ), apparent density of the adsorbent (ρ_p), and particle radius (R). The

adsorption resistance is represented by δ_a, the intraparticle resistance by δ_i, and the external diffusion resistance by δ_e. The mass transfer coefficient, k_f, may be related to the molecular diffusivity, D_{AB}, at low Reynolds number by (13):

$$k_f R = D_{AB} \tag{19}$$

By integrating the experimental elution curve, the first and second moments may be obtained. From the first moment, the value of K_A may be found using Equations 12 and 14 since all other parameters are independently determined. Assuming that the rates of external mass transfer and adsorption are much faster than pore diffusion, D_e may be calculated from the second moment if the axial dispersion coefficient is assumed to have the same value as for a packing of solid particles.

Haynes and Sarma [13] describe first and second moment expressions for the same bidisperse pore model employed by Smith and Williams [9]. The model assumes that the porous solid is a sphere of radius R which is formed from many microporous particles of radius R_x. The void space surrounding the microparticles forms the macropores and has a diffusivity of D_y. The diffusivity in the micropores is D_x. Assuming adsorption is negligible, the unipore effective diffusivity, D_e, obtained from Equations 9-19 may be related to the macropore and micropore diffusivities and porosities:

$$\frac{1}{D_e} = \frac{1}{D_y} + \frac{(1-\theta_y)\,\theta_x^2\,R_x^2}{R^2\,[\theta_y+(1-\theta_y)\theta_x]^2\,D_x} \tag{20}$$

By measuring the unipore effective diffusivity over a range of particle sizes and plotting $1/D_e$ versus $1/R^2$, a straight line should be obtained and evaluation of the intercept will give D_y and the slope will give D_x/R_x^2 assuming that the micropore and macropore porosities can be measured. For coal, R_x cannot be directly measured and therefore, only D_x/R_x^2 may be found.

The experimental apparatus used in this work resembles a gas chromatograph and a schematic diagram of the apparatus is shown in Figure 1. The helium carrier gas is fed into the system via two-stage regulators to ensure minimum flow rate flucuations. The gas flow rates are controlled with Nupro needle valves. Sample injection is accomplished by passing the carrier and tracer gases through opposite ports of a Valco 8-port valve having a 0.10 cm^3 sample loop. To minimize entrance effects, this valve is located immediately before the column entrance. Tracer gases are UHP methane and nitrogen. Injection of the tracer is accomplished by switching two solenoid valves which control the flow of air to the Valco valve actuator. The carrier gas flow rate is determined using a soap film flow meter and, because this flow rate measurement is essential in the analysis, ten readings are taken and the average is used. The standard deviation of these ten readings is less than 1% of the mean value.

The column is fabricated from 1/4 inch stainless steel tubing with an inner diameter of 0.538 cm. To minimize end effects, a column length of 51.36 cm is used. The distance between the sampling valve and tube was kept short and the connection made with 0.159 cm OD stainless steel tubing to minimize dispersion in the entrance region of the column.

The thermal conductivity detector(TCD) system consists of a GOW-Mac Inc. thermistor detector and a GOW Mac power supply/controller. The thermal conductivity detector is coupled directly to the column outlet to minimize dispersion at the column outlet. The detector utilizes two 8 KΩ thermistors which are operated at 8 mA DC current. The internal cell volume is 0.025 cm^3, which minimizes the time lag due to cell mixing. The analog signal from the power supply/controller (0-1V DC) is digitized using a fast-response Keithley #192 multimeter (60 readings/sec). The digitized signal is sent

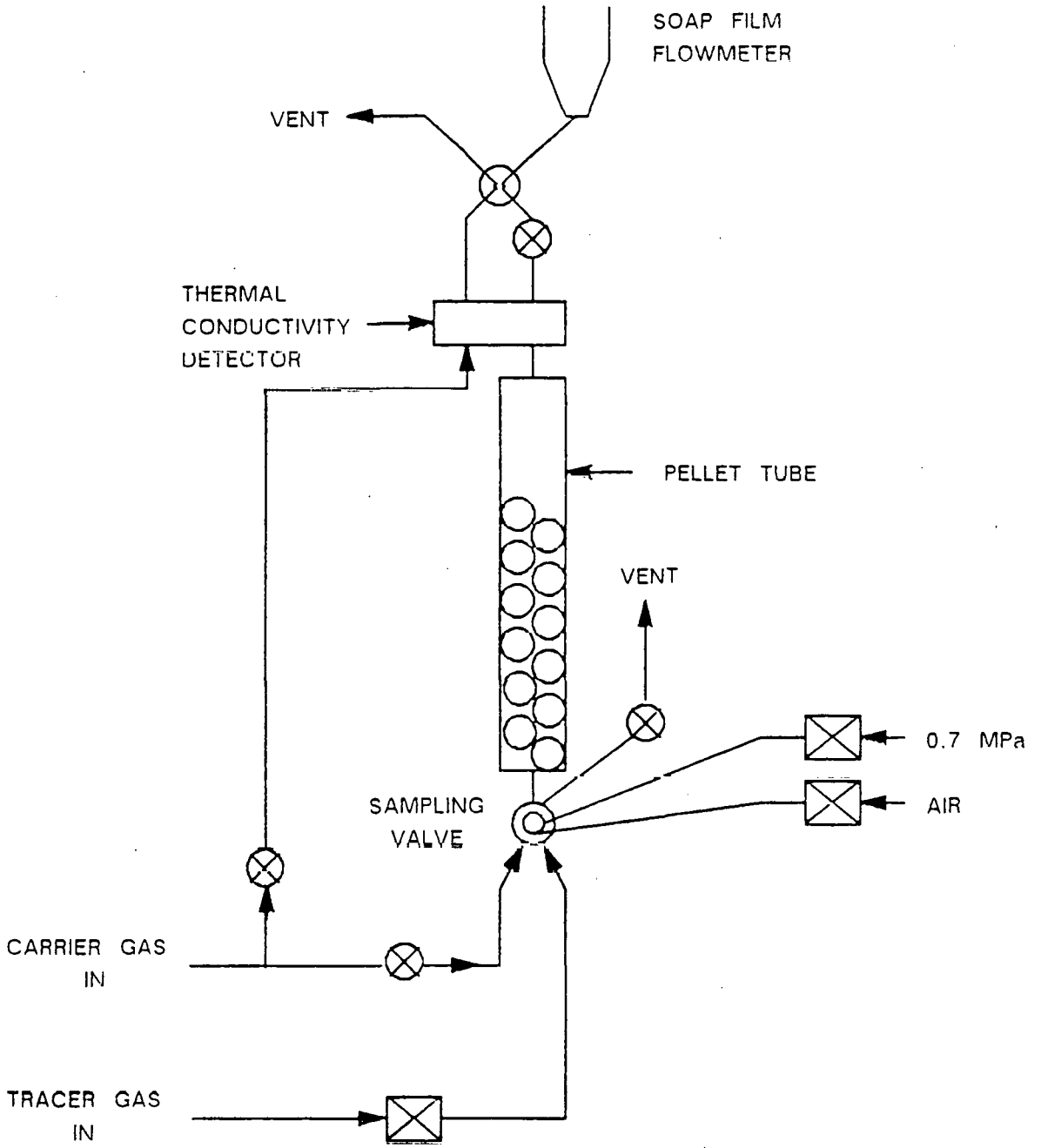

Figure 1. Schematic Diagram of Experimental Apparatus

via IEEE-488 instrument bus to an HP-85A microcomputer for data reduction. The elution curve is integrated using the trapezoidal rule.

Eight coal samples with well-defined history and representing a range of rank and geographic location were obtained from the Penn State Coal Data Bank (PSOC coals). Table 1 lists each coal with its corresponding rank, geographic location and physical properties. Particle sizes that were used are: 0.152+/-0.018 cm, 0.110+/-0.013 cm, and 0.055+/-0.007 cm. These sizes were chosen to minimize pressure drop. For PSOC-1354 and PSOC-869 coal samples, three smaller particle sizes were used to extend the size range. These sizes were: 0.023+/-0.003 cm, 0.011+/-0.001 cm, and 0.005+/-0.001 cm. The coal samples were dried at 353 to 393 K overnight in air. After drying, the samples were packed into the column and the column was reattached to the apparatus. Helium then flowed through the column at 298 K for an hour to purge the system of all extraneous gases.

The range of bed void fractions (α), 0.58 - 0.36, among the coals can be attributed to different particle shapes and size distributions. The large α values were obtained for the largest particle sizes as would be expected since particle size and tube size are on the same order. The column was repacked with PSOC-128, and PSOC-139 for d_p = 0.110 cm to demonstrate the reproducibility of α. For PSOC-128 the second packing had a bed void fraction equal to 0.372 compared to 0.363 for the first packing and for PSOC-139 the second packing had a bed void fraction equal to 0.481 compared to 0.484 for the first packing.

The column pressure drop was calculated using the Ergun equation [14] For the smallest particle size, closest packing, and highest flowrate, the experimental conditions where one would expect pressure drop to be the highest, ΔP was equal to 0.049 psi. Despite being an upper limit, this pressure drop is significantly low and it was assumed that no correction was

COAL	LOCATION	RANK	N_2 SA (m^2/g-DAF)	CO_2 SA (m^2/g-DAF)	N_2 PV (cm^3/g-DAF)	He ρ (g/cm^3-Dry)	Hg ρ (g/cm^3-Dry)
88	Zap, ND	Lignite A	3.0	130.5	0.032	1.62	1.43
139	Darco, TX	Lignite A	6.1	126.6	0.056	1.50	1.40
856	Juanita C, CO	HVBB	2.2	122.7	0.052	1.60	1.25
859	Dakota, CO	HVCB	2.4	108.4	0.034	1.60	1.32
1354	Illinois #6, IL	HVCB	22.0	163.6	0.190	1.46	1.12
852	D Seam, CO	HVBB	19.3	146.3	0.034	1.61	1.31
128	Lower Kittanning, PA	LVB	1.2	133.9	0.052	1.76	1.30
869	Primrose, PA	Antracite	5.0	104.2	0.049	1.92	1.58

Table 1. PSOC coals and physical properties in order of increasing carbon content.

needed for the measured volumetric flow rate. For PSOC-1354 and PSOC-869 coal samples, three smaller particle sizes were used and the highest calculated ΔP was 0.421 psi.

RESULTS AND DISCUSSION

For the PSOC-856 coal, experiments at five different flow rates were conducted and at each flow rate five runs were done. Typical elution curves corresponding to two different volumetric flow rates are shown in Figure 2. The first absolute moment, μ_1', was reproducible within 1%, and the second central moment, μ_2, was reproducible within 5%. Since the reproducibility of the experiments was demonstrated for the PSOC-856 coal, the remaining experiments were conducted at only 3 or 4 different flow rates and only 3 or 4 runs were done at each flow rate. For each run, μ_1' was reproducible within 1% for all the coals and both nitrogen and methane tracers. The second central moment was reproducible within 5% for all of the coals except for the PSOC-852, PSOC-1354, and PSOC-139 coals with methane as the tracer gas. The tailing on the elution curves for these coals was so significant that μ_2 could not be reproduced. Therefore, effective diffusivities for methane in these coals could not be determined. This tailing effect is an indication that methane adsorbs onto these coals and will be discussed subsequently.

For all eight coals, the unipore effective diffusivity for nitrogen has been determined as a function of carrier velocity and particle size. In principle, D_e should be independent of particle size and velocity. The effect of changing velocity on D_e was found to be insignificant but a major (and somewhat unexpected) particle size dependence was observed for all eight coals. Typical results are presented in Figure 3 using the PSOC-1354 coal as an example. This major variation of D_e (two orders of magnitude)

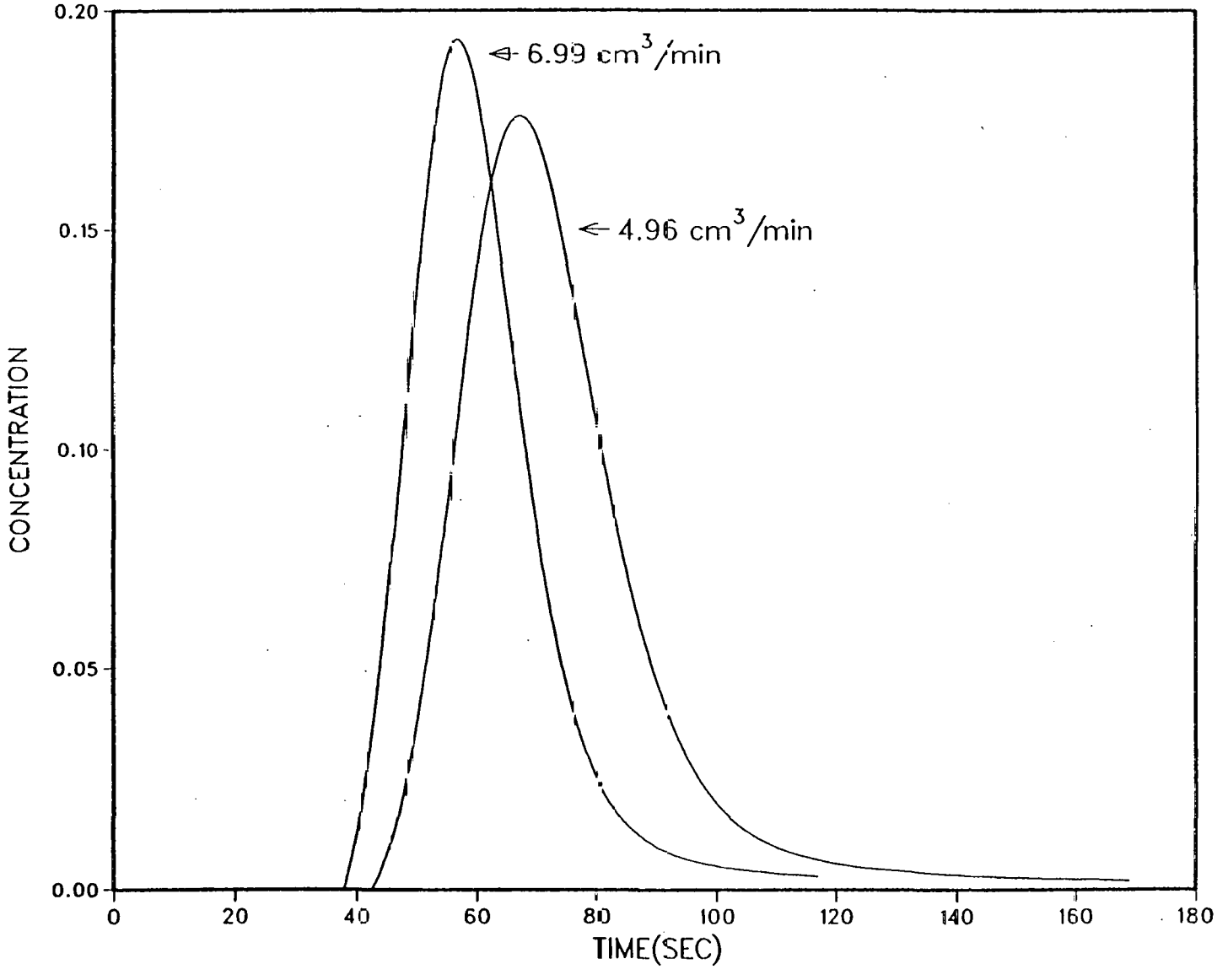

Figure 2 Typical elution curves for FSOC-856 coal and two carrier flow rates.

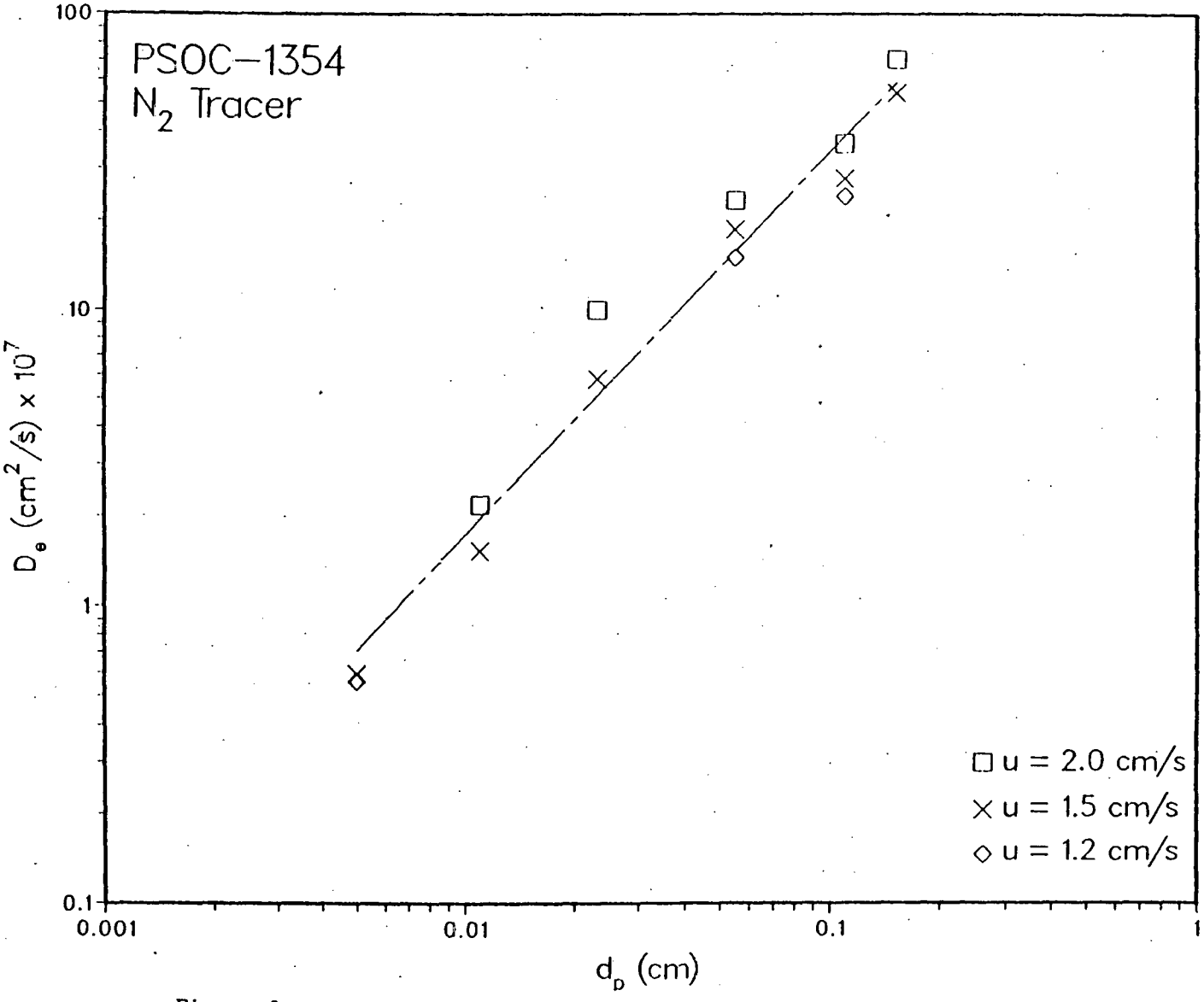

Figure 3 Variation of effective diffusivity as a function of particle size and carrier velocity for the PSOC-1354 coal.

with particle size is the result of the complex pore structure of coal and the failure of the unipore model to describe transport in coal.

For nitrogen effective diffusivities measured for a fixed particle size and flow rate, attempts were made to correlate the magnitude of D_e with various pore structure parameters. These parameters included various definitions of the mean hydraulic radius (2PV/SA). Only by employing the hydraulic radius of the macropores (i.e., by using the surface area and pore volume determined from nitrogen adsorption/condensation at 77 K) was any general trend noted. This result is presented in Figure 4 for three different particle sizes and eight coals. As expected, increasing pore radius resulted in increasing diffusivity. On first thought, this would suggest that transport is controlled by diffusion in macropores. If transport is macropore diffusion controlled, than a linear plot of D_e/θ should be linear with slope proportional to the inverse of the tortuosity factor. If this is attempted, the plot shows significant nonlinearity and results in tortuosity factors on the order of 100-1000. These τ values are to large to be physically significant.

The fact that the slope of a line fit to the data of Figure 3 is approximately two implies that the bidisperse pore model [9,13] described earlier may be appropriate. Presented in Figure 5 is a log-log plot of inverse effective diffusivity versus inverse particle radius squared for the PSOC-869 coal for both nitrogen and methane tracers. The fact that the data in this plot is linear for over three orders of magnitude in $1/R^2$ and has a slope near one is quite interesting. Linear behavior was noted for all eight coals when the results were presented on a linear $1/D_e$-$1/R^2$ plot although for most samples, only three particle sizes were studied (such as the methan eresults presented in Figure 5). As discussed previously with regards to Equation 20, the slope and intercept of these plots may be

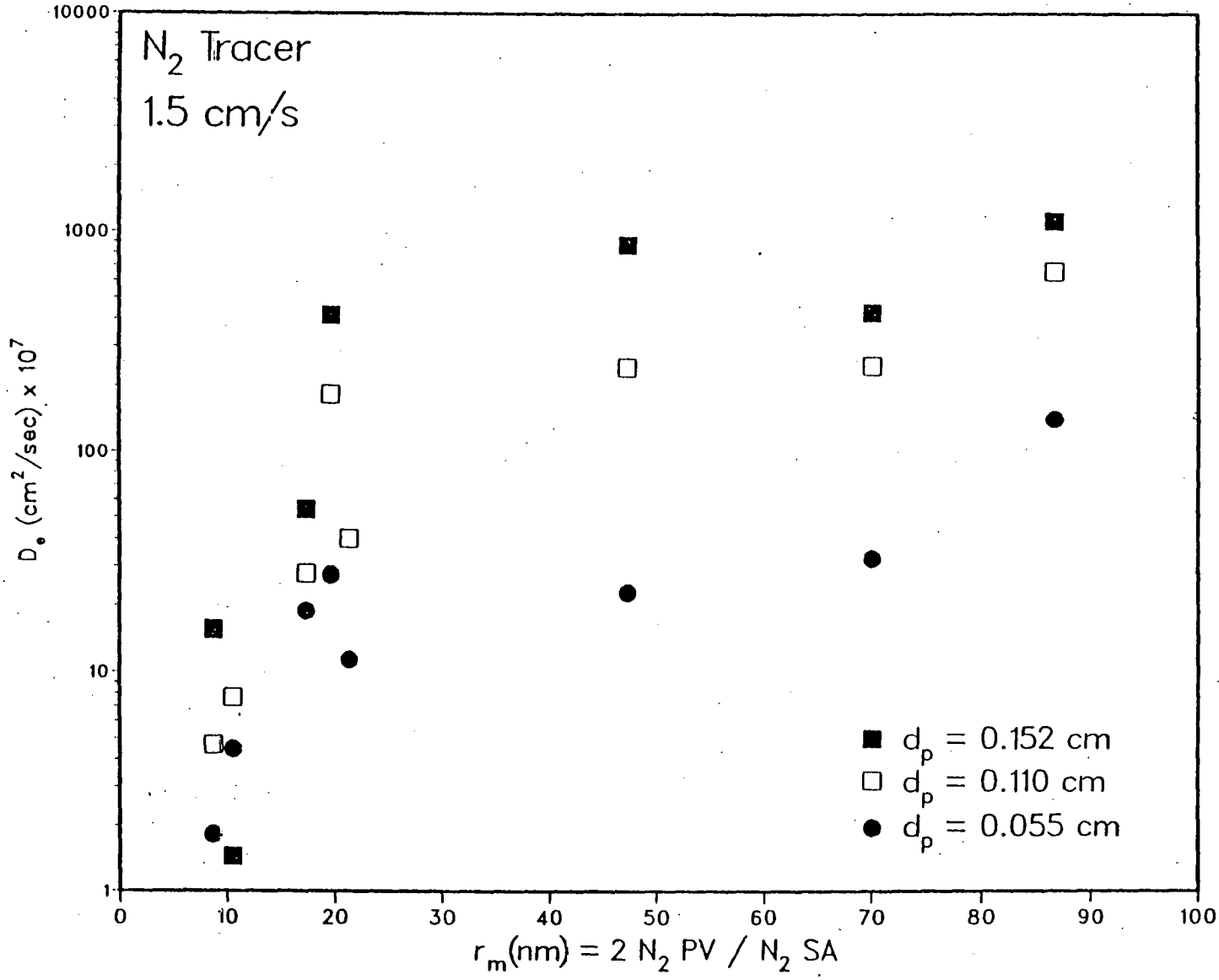

Figure 4 Variation of nitrogen effective diffusivity with macropore hydraulic radius for all eight coals.

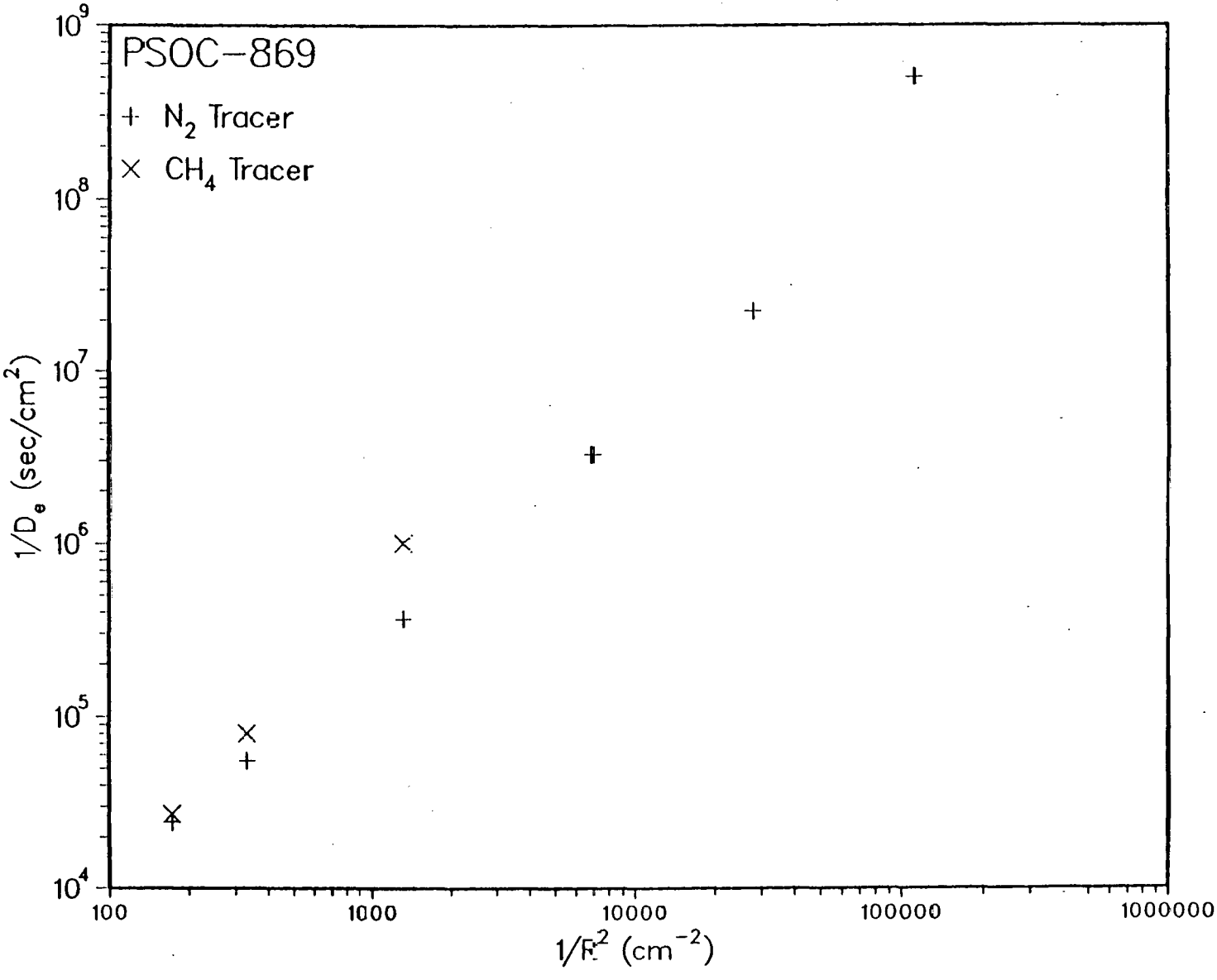

Figure 5 $1/D_e$ versus $1/R^2$ plot for PSOC-869 coal.

analyzed top obtain the macropore diffusivity, D_y, and the micropore diffusion group, D_x/R_x^2. The intercept is equal to $1/D_y$ and the slope is $(1-\theta_y)\theta_x^2R_x^2/[D_x(\theta_y+(1-\theta_y)\theta_x^2)]$. Therefore, in order to obtain the desired micropore diffusion parameter, D_x/R_x^2, both the micropore and macropore porosity must be obtained. We have assumed that the pore volume obtained by nitrogen condensation at 77 K is a measure of the volume associated with macropores. In addition, the total porosity of the coal particles, θ, may be obtained from the densities measured via helium and mercury displacement. The micopore porosity, θ_x, may be obtained from θ and θ_y. Table 2 contains values of θ, θ_x, θ_y for all eight coals as well as the micropore diffusion group, D_x/R_x^2, for both nitrogen and methane. Several points in Table 2 should be noted. For the PSOC-139, a Texas lignite, the macropore porosity was larger than the helium/mercury total porosity and thus, micropore porosity and diffusion parameters could not be determined. This is probably the result of different drying history for the same material before the different analysis or sample to sample variation. Further evidence for the validity of the macropore porosity values is obtained from the general trend which is observed between θ_y and the nitrogen surface area. Macropore diffusivities are not reported in Table 2 since the magnitude of $1/D_y$ is much less than $1/D_e$ for the particle sizes which we used. To obtain accurate D_y would require measuring D_e for larger particles which we were unable to accomplish in our experimental apparatus. However, from a practical viewpoint, the micropore diffusivity is the parameter of interest.

It was the original intent of the study to try and relate diffusion parameters, such as D_x/R_x^2, to pore structure parameters. Figure 6 is a log-log plot of the micropore diffusivity as a function of the micropore porosity for both nitrogen and methane diffusion. A general trend of increasing micropore diffusion with increasing porosity is observed. A

COAL	Θ	Θ_y	Θ_x	$\frac{D_x}{R_x^2}$ (N_2)	$\frac{D_x}{R_x^2}$ (CH_4)
88	0.117	0.070	0.05	2.76×10^{-4}	7.46×10^{-5}
139	0.067	0.092	0	---	----
856	0.219	0.065	0.165	4.39×10^{-4}	1.78×10^{-4}
859	0.175	0.111	0.072	5.83×10^{-4}	1.23×10^{-4}
1354	0.233	0.213	0.025	1.40×10^{-5}	NA
852	0.186	0.110	0.085	4.74×10^{-5}	NA
128	0.261	0.068	0.207	1.06×10^{-2}	2.31×10^{-3}
869	0.177	0.077	0.108	7.57×10^{-5}	3.87×10^{-4}

Table 2. Porosities and micropore diffusion parameters for eight PSOC coals.

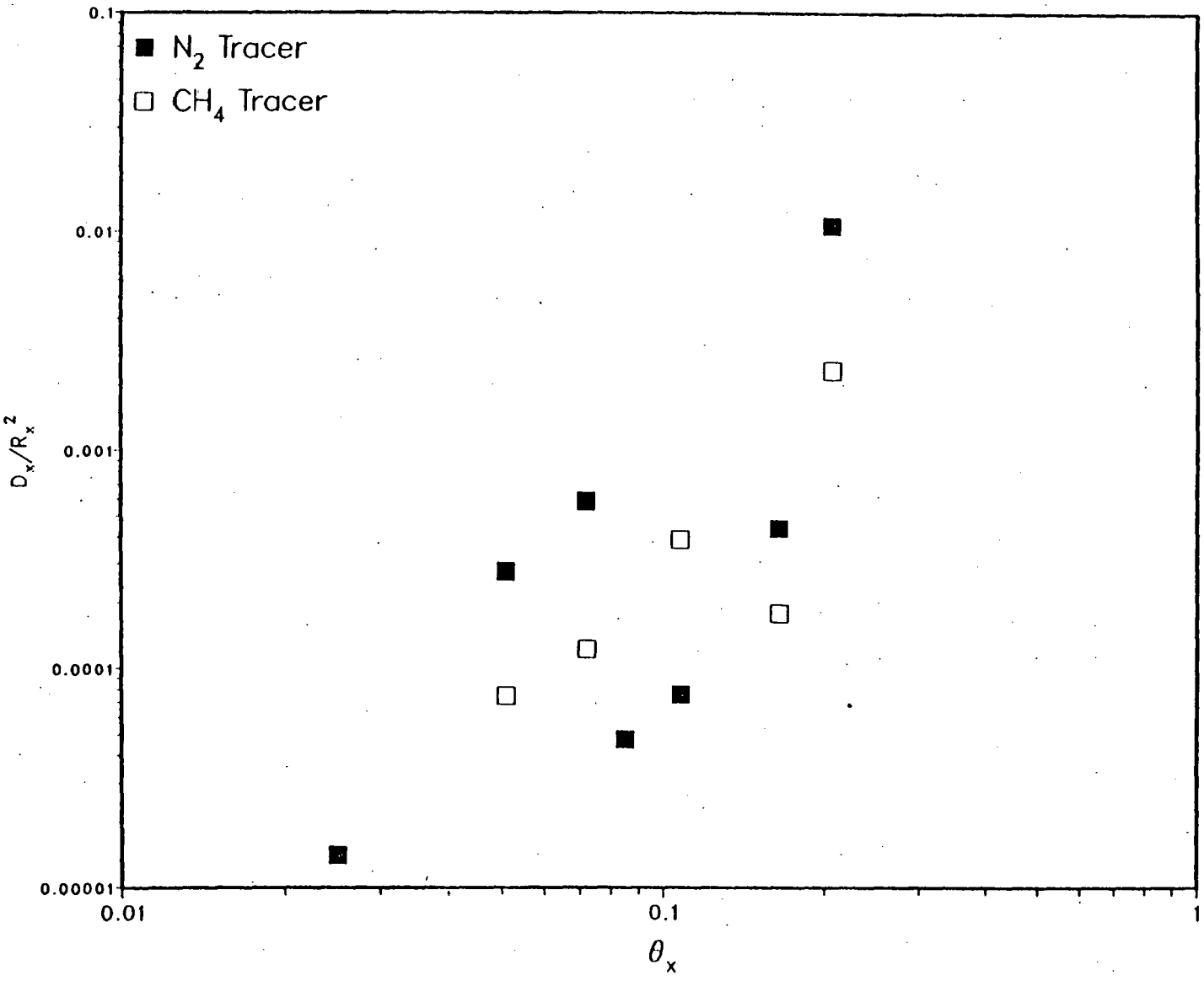

Figure 6 Variation of micropore diffusion group with micropore porosity.

least squares fit to this data indicates a slope of 2.2 (i.e., that D_x/R_x^2 is proportional to $\theta_x^{2.2}$). This can be explained by remembering that D_x is an effective diffusivity which contains a porosity, tortuosity and pore diffusivity ($D_x = D_{pore}\theta_x/\tau$). Assuming that the micopore pore diffusivity is constant for all coals (this is certainly not true since the micropore size will vary), the 2.2 power can be explained by defining τ as $1/\theta_x^{1.2}$. This is very close to the value of $1/\theta$ which is often taken as an approximate value of τ [14].

Only three coals showed significant adsorption (K_A) of the tracers from the first moment data analysis. These three coals were the PSOC-1354, PSOC-139, and PSOC-852. These three coals can be singled out due to their high N_2 surface areas relative to the other coals. It seems that a high N_2 surface area is necessary for adsorption to occur. Figure 7 shows K_A as a function of N_2 surface area for all the coals at a particle size of 0.055 cm. Although PSOC-852 has a higher N_2 and CO_2 surface area than PSOC-139 this is not reflected directly by the magnitude of K_A, which indicates that as expected, adsorption is a function of the chemical nature of the surface in addition to the N_2 surface area. Figure 8 shows a plot of K_A versus particle size for both nitrogen and methane tracers. From this plot it is evident that as particle size decreases the adsorption coefficient increases. This effect does not match the prediction of the bidisperse pore model since according to that model, the value of K_A should be independent of particle size. However, one would not necessarily expect such a simple model to describe all the phenomena in a complex material such as coal.

NOMENCLATURE

A = Area under the elution curve

c = Tracer concentration in the interparticle space

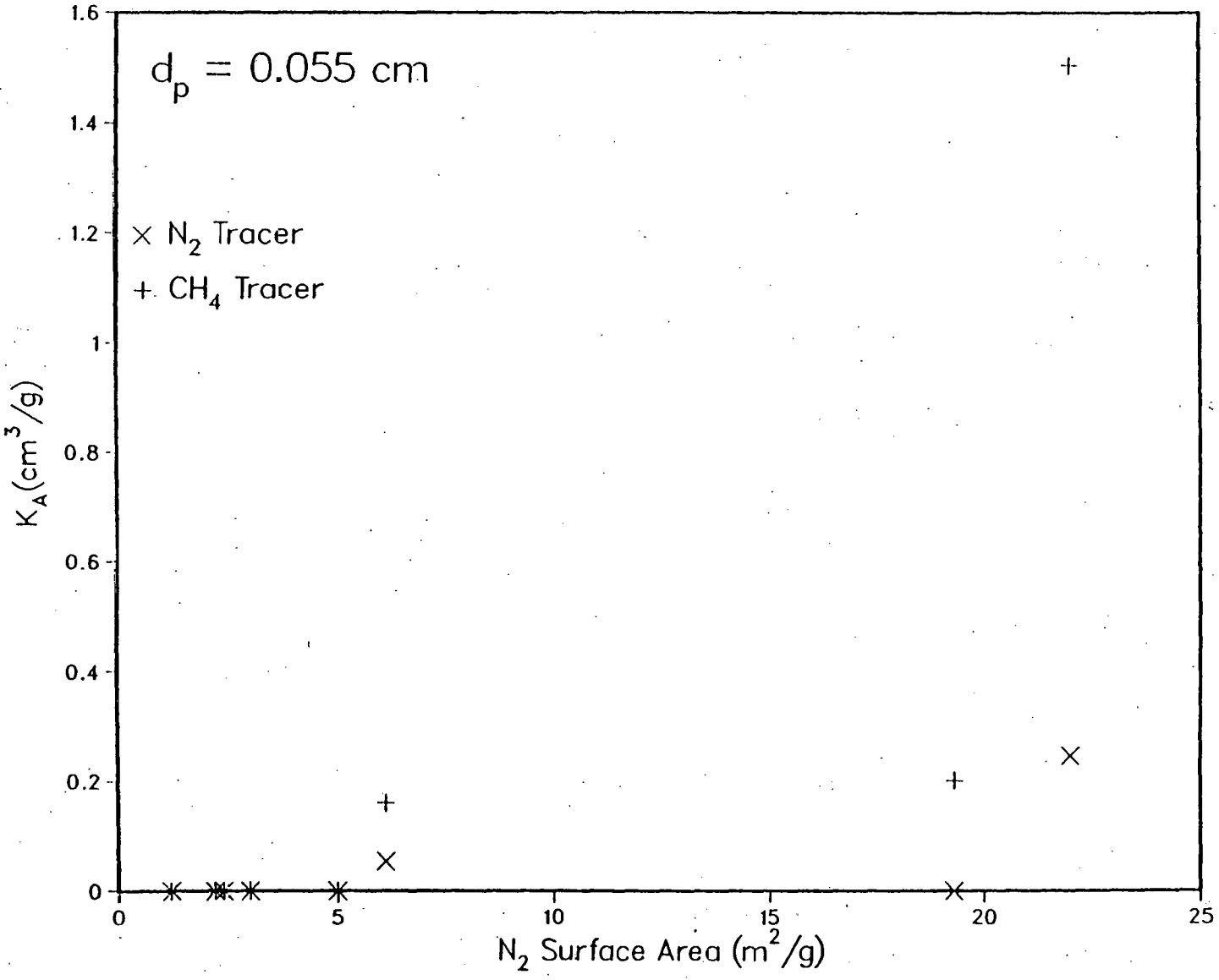

Figure 7 Methane and nitrogen adsorption constants as a function of nitrogen surface area.

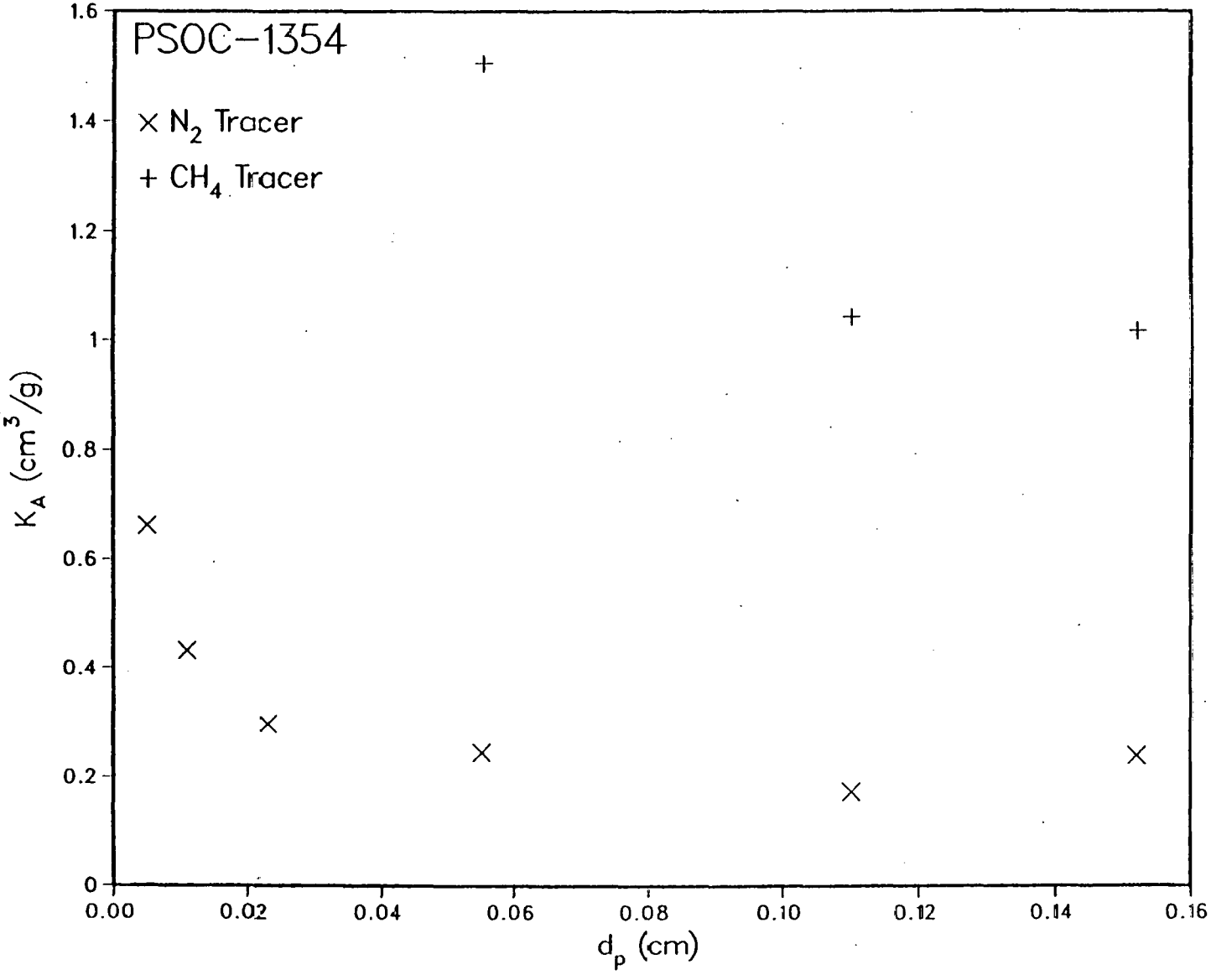

Figure 8 Variation of adsorption constants as a function of particle size for the PSOC-1354 coal.

c_i = Tracer concentration in the pore space

c_{ads} = Concentration of the adsorbed gas

c_o = Inlet tracer concentration

D_e = Effective diffusivity

D_L = Axial dispersion coefficient

D_M = Molecular diffusivity

D_x = Micropore effective diffusivity

D_y = Macropore effective diffusivity

k_{ads} = Adsorption rate constant

k_f = Mass transfer coefficient

K_A = Adsorption equilibrium constant

L = Column length

n = Empirical constant of Airey [4]

N_x = Flux of diffusing gas

PV = Pore volume

r = Spatial coordinate in the absorbent

R = Paricle radius

SA = Surface area

t = Time

t_o = Pulse duration

T_o = Empirical constant of Airey [4]

u = Carrier gas velocity

V_t = Quantity of gas adsorbed at time t

V_∞ = Quantity of gas adsorbed at equilibrium

z = Length coordinate of the adsorbent bed

α = Interparticle void fraction in the adsorbent bed

θ = Internal porosity of the adsorbent

θ_x = Micropore porosity

θ_y = Macropore porosity

δ_o = Defined in Equation 14

δ_1 = Sum of resistances defined in Equation 15

δ_a = Adsorption resistance defined in Equation 16

δ_e = External resistance defined in Equation 17

δ_i = Internal resistance defined in Equation 18

μ_1 = First absolute moment

μ_2 = Second central moment

τ = tortuosity factor

REFERENCES

[1] Ruppel, T.C., Grein, C.T. and Bienstock, D., "Adsorption of Methane/Ethane Mixtures on Dry Coal at Elevated Pressure," Fuel, 51, p. 247, (1972).

[2] Sevenster, P.G., "Diffusion of Gases Through Coal," Fuel, 38, p.403, (1959).

[3] Thimons, E.D., and Kissell, F.N., "Diffusion of Methane Through Coal," Fuel, 52, p. 274, (1973).

[4] Airey, E.M., "Gas Emission from Broken Coal: An Experimental and Theoretical Investigation," I. J. of Rock Mech and Mining Sci., 5, p. 475, (1984).

[5] Smith, D.M., and Williams, F.L., "Diffusion Models for Gas Production from Coal: Application to Methane Content Determination," Fuel, 63, p. 251, (1984).

[6] Nandi, S.P. and Walker, P.L., "The Diffusion of Nitrogen and Carbon Dioxide from Coals of Various Ranks," Fuel, 43, p. 385, (1964).

[7] Nandi, S.P. and Walker, P.L., "Activated Diffusion of Methane in Coal," Fuel, 49, p. 309, (1970).

[8] Gan, H., Nandi, S.P. and Walker, P.L., "Nature of the Porosity in American Coals," Fuel, 51, p. 272, (1972).

[9] Smith D.M. and Williams F.L., "Diffusion Models for Gas Production from Coal: Determination of Diffusion Parameters," Fuel, 63, p. 256, (1984).

[10] Gallegos, D.P., Smith D.M., and Stermer, D.L., "Pore Structure Analysis of American Coals," CHARACTERIZATION OF POROUS SOLIDS, Unger, K.K, Rouquerol, J., Sing, K.S.W., Kral, H., editors, Elsevier, p. 509, (1988).

[11] Glaves, C.L., Davis, P.J., Gallegos, D.P., and Smith, D.M., "Pore Structure Analysis of Coals via Low Field Spin-Lattice Relaxation Measurements," Energy & Fuels, in press.

[12] Schneider P. and Smith J.M., "Adsorption Rate Constants from Chromatography," AIChE J., 14, p. 762, (1960).

[13] Haynes, H.W. and Sarma, P.N., "A Model for the Application of Gas Chromatography to Measurement of Diffusion in Bidisperse Structured Catalysts," AIChE, 19, p. 1043, (1973).

[14] Forment, G.F., and Bischoff, K.B., Chemical Reactor Analysis and Design, Wiley, (1979).

2.2 NMR AND PORE STRUCTURE STUDIES

INTRODUCTION

It is usually recognized that a variety of analysis schemes are required to probe the pore structure of coal over the entire pore size range of interest. This may imply the use of gas adsorption (nitrogen and carbon dioxide), mercury porosimetry, small-angle x-ray scattering (SAXS), molecular probes, and/or density measurements (helium and mercury displacement). All of these characterization techniques suffer from inherent problems such as a limited pore size range, errors due to network/percolation effects, the necessity of pore shape assumptions, and/or sample changes during analysis. In this work, we explore the use of low-field NMR spin-lattice relaxation measurements as a pore structure analysis technique for coal. A fluid contained in a pore will exhibit a shorter spin-lattice relaxation time, T_1, than the same fluid in bulk solution. In the model we present, this reduction in T_1 is based on a difference in surface affected and bulk fluid relaxation rates within a pore, in combination with fast diffusional exchange between these fluid regions. T_1 can thus be related to the pore size. This analysis scheme has several advantages such as finding the actual hydraulic radius of the pore with no shape assumption (for pores of radius $> \approx 5$ nm), applicability to a wide pore size range from micropores to pores greater than 1 μm, and independence of network/percolation effects.

In applying spin-lattice relaxation measurements to coal pore size determination it is assumed that the fluid sorbed into the coal is a result of condensation in pores, and that this sorption does not alter the pore structure. This assumption is best for high rank coals and becomes questionable for low rank coals which have a high degree of oxygen functionality and are known to strongly interact with water and other organic fluids. The interpretation of NMR measurements for low rank coals

thus has the potential of being more complex than the treatment presented in this paper, i.e. that of a simple porosity model, and caution should be exercised when infering quantitative pore structure information in these cases.

BACKGROUND

Although the adsorption of nitrogen at 77 K is the standard method of surface area determination, Anderson and co-workers [1] demonstrated that coal surface areas determined via this approach are smaller than expected. Marsh and Siemieniewska [2] have shown that analysis via the Dubinin-Radus-kevich equation of carbon dioxide adsorption in the temperature range of 195 to 293 K results in the measurement of the "total" surface area. It is postulated that the reason for the much lower nitrogen surface areas is activated diffusion which limits the ability of nitrogen at 77 K to access the surface area in pores with radii less than approximately 1-2 nm.

Although the use of nitrogen and carbon dioxide surface areas will give some information concerning the relative ratio of surface area in macro-pores/mesopores to the total surface area, little pore size distribution information is obtained. Obtaining pore size distribution information implies the use of either nitrogen condensation ($1<r<100$ nm) or mercury poro-simetry (1.5 nm$<r<10$ μm). Zwietering and van Krevelen [3] used mercury intrusion measurements over the pressure range of 15 to 15,000 psia in an attempt to determine the pore size distribution of a single coal. The volume-pressure curve was linear between 7,500 and 15,000 psia which the authors attributed to sample compression. The authors obtained a compres-sibility from the slope of the curve in this linear region which was used to correct the remainder of the intrusion curve for compression. Although the

particle size of the sample was not given, it is clear that intrusion at low pressures was the result of mercury filling in surface roughness and in the void volume surrounding the particles. This apparent intrusion was not discussed and was attributed solely to pore filling. Gan, Nandi and Walker [4] studied a number of American coals using nitrogen and carbon dioxide adsorption, nitrogen condensation, helium density and mercury porosimetry. Pore volumes in the pore size range which overlap for nitrogen condensation and mercury porosimetry indicated a larger pore volume from porosimetry as compared to condensation. This was probably the result of not attempting to make any correction for the effects of compression. Porosimetry at lower pressures, for which compression is not significant, indicated very little pore volume in the macropore size range. The volume associated with mesopores could not be determined because of compression effects, and with micropores could not be determined because of the upper pressure limit of the measurements. Sixteen coals have been analyzed via mercury porosimetry by Toda and Toyoda [5]. They concluded that no pores exist in the size range of approximately 20 to 7.5 nm (the lower limit of the measurements) and that all observed intrusion in that pore size range was due to sample compression. The effects of void filling around the particles and in surface roughness at low pressures was not discussed. Coal compressibility, found from the slope of the intrusion curve at high pressure, was found to be independent of carbon content which implies that for coals with pores in the size range of 3 to 20 nm, compression corrections cannot be attempted. A similar finding has been reported by Debelak and Schrodt [6] for four Kentucky coals. In contrast, Spitzer [7] compared mercury porosimetry and small angle x-ray scattering and concluded that when porosimetry is corrected for compression, the two methods are in good agreement. However,

in that work, the compressibility was assumed to be the same for all 20 coals studied which represented a broad range of rank. This assumption is certainly not supported by other investigators [5,6]. Since the pore size distribution of coals is apparently quite broad and since the quantity of pore volume in macropores and mesopores is usually small (<0.05 cm^3/g), the errors associated with this compressibility assumption will completely distort the calculated pore size distribution.

In addition to compression questions for the application of porosimetry, the effect of sample particle size may also be significant. This effect has been demonstrated by Gallegos, Smith and Stermer [8] using a range of particle sizes. That work illustrates the problems associated with isolating the effects of void filling around the particles, surface roughness filling, sample compression, network/percolation effects, and the desired pore filling. In summary, mercury porosimetry should only be applied to coal samples with great care and a range of particle sizes should be considered as a means of ascertaining the magnitude of pore filling.

A series of NMR investigations of water contained in coal have been presented by Lynch, Webster and co-workers [9-12]. In a study of brown coal [10], spin-lattice relaxation experiments indicated nonexponential relaxation which they postulated to be the result of cross-relaxation with protons in the coal matrix. The possibility of this non-exponential decay resulting from a distribution of pore sizes was not considered. The applicability of pulse α-NMR for moisture content determination was demonstrated for eight coals samples [11]. More recently, Lynch and coworkers [12] have shown using raw and deashed coals that spin-spin relaxation is essentially independent of the paramagnetic impurities for coals.

The use of NMR spin-lattice relaxation measurements as a pore structure probe was recognized by researchers in the field of petroleum reservoir logging. In principle, a fluid confined in a pore will relax at a faster rate than the same fluid in the bulk. The characteristic spin-lattice relaxation decay time, T_1, in a pore is usually assumed to be described by the two-fraction, fast exchange model [13] which treats the fluid in a pore as existing in two phases, a surface-affected phase with characteristic decay time, $T_{1surface}$, and a phase with the same properties as the bulk fluid. If diffusion between the two phases is fast as compared to the intrinsic relaxation rates, the observed relaxation is a function of the relative fractions of the two phases:

$$1/T_1 = f_b/T_{1b} + f_s/T_{1surface} \quad (1)$$

If the pore size is relatively large (i.e., $r_p > 5$ nm), the volume of the surface phase is much less than the bulk phase and Equation 1 may be written in terms of the surface area to volume ratio of the pore:

$$1/T_1 = 1/T_{1b} + SA/PV\ (1/T_{1s}) \quad (2)$$

T_{1s} is now the ratio of $T_{1surface}$ and the thickness of the surface-affected phase. Previous work by Woessner [14] and Almagor and Belfort [15] indicates that the thickness of the surface-affected phase is on the order of one to two monolayers. For pore structure analysis, $T_{1surface}$ and the surface layer thickness are usually not determined separately. Instead, the pore radius, r_p, is defined as the hydraulic radius, 2PV/SA, and is related to the measured T_1 by:

$$1/T_1 = \alpha + \beta/r_p \quad (3)$$

where α is equal to $1/T_{1b}$ and is determined from a T_1 experiment on the bulk fluid. The constant β is a measure of the surface-enhanced relaxation and is a function of fluid/adsorbate, field strength, temperature, and surface

chemistry. In actuality, α is probably different from that measured via an independent experiment on bulk fluid, this being due to an indeterminant amount of impurities dissolved into the pore water of sorbed systems from the pore matrix material. The error made in determining α becomes insignificant, however, because of the fact that very small T_1 values are observed for coal samples, thus making α itself an insignificant parameter in Equations 2 and 3.

Equations 2 and 3 are valid for pores with radius greater than approximately 5 nm and imply that no assumption concerning pore geometry has been made. For mesopores and micropores, a pore geometry must be be assumed to relate the relative fractions of surface and bulk phases to the pore size. This problem was addressed by Gallegos, Smith and Brinker [16] for pore models including flat plate, cylinder, spherical cavity, and the pore space surrounding solid spheres. By using an assumption concerning pore geometry, the lower limit of NMR pore size analysis may be extended from approximately 5 nm to approximately 0.5 nm. For this micropore analysis an additional parameter ,Δ, the thickness of the surface-affected phase, is required and is on the order of one to two monolayers ($\approx$ 0.3 nm). In addition, the fraction of the total pore volume which exists in pores with radii less than 0.5 nm may be determined, but no size distribution information may be obtained for those pores.

For bulk fluid or a porous solid with a single pore size, the return to equilibrium of the magnetization vector at time τ during an inversion recovery spin-lattice relaxation experiment is given by:

$$M(\tau) = M_0 [1-2\exp(-\tau/T_1)] \qquad (4)$$

For a porous solid with a distribution of pore sizes, the observed relaxation, $M(\tau)$, is a function of the relative volume and size of all pores. Therefore, Equation 4 must be summed over the T_1 distribution, $f(T_1)$:

$$M(\tau) = M_0 \int_{T_{1min}}^{T_{1max}} [1-2\exp(-\tau/T_1)]\, f(T_1)\, dT_1 \qquad (5)$$

The problem is to extract the desired T_1 distribution, $f(T_1)$, from a series of measurements of $M(\tau)$. $f(T_1)$ is related to the pore size distribution via Equation 3 for materials with pore sizes greater than approximately 5nm. A more complicated equation is used to relate the two for materials including pores smaller than 5 nm [16]. Equation 5 is a Fredholm integral equation of the first kind which forms the basis of the "ill-posed" nature of this inversion problem. Munn and Smith [17] used a non-negative least squares (NNLS) approach to obtain discrete distributions which approximated the actual continuous distribution. This approach was satisfactory for a solid with one or more narrow peaks in the T_1 distribution. However, for a material like coal, a broad distribution can be anticipated. More recently, several investigators [18,19] have used the method of regularization to obtain continuous T_1 distributions for the purpose of pore structure analysis. The problem with the regularization approach is obtaining a proper value of the smoothing parameter, δ. The optimum value of δ will depend upon both $f(T_1)$, which isn't known, and the magnitude of the experimental error in the $M(\tau)$ data set, which may be estimated. In previous work [18,19], the method developed by Butler and co-workers [20] was used to determine δ_{opt} given an estimate of the measurement precision. Using a series of model porous solids such as controlled pore glass and random

packings of uniform spheres, Gallegos and Smith [19] showed that the NMR-derived pore size distributions agreed well with the expected distribution of hydraulic radius.

For pore structure analysis, the value of the surface interaction parameter, β, must be determined for a particular fluid, temperature, proton frequency, and solid surface chemistry. Gallegos and co-workers [21] determined β values by using solids of similar surface chemistry and known pore size distribution. However, for most materials, these calibration porous solids are not available and NMR-derived pore structure information becomes dependent on the errors associated with conventional pore structure analysis. More recently, Davis and co-workers [22] have simplified the β determination process. In that work, the sample was not completely saturated, but rather a quantity of fluid was adsorbed on the sample and the amount adsorbed determined gravimetrically. If the specific surface area (SA) of the sample is known, the fraction of fluid in the surface phase is given by:

$$f_s = \Delta \; SA \; C \tag{6}$$

where C is the mass of sample per unit volume of fluid. Equations 1 and 6 may be combined:

$$1/T_1 = 1/T_{1b} + SA \; C \; [\Delta/T_{1surface} - \Delta/T_{1b}] \tag{7}$$

Since T_{1b} is usually several orders of magnitude larger than $T_{1surface}$ in low field applications, the second term in the brackets of Equation 7 can be neglected. Using the definition of β, Equation 7 may be rewritten:

$$\beta = 2 \; [1/T_1 - \alpha \;] \; / \; [SA \; C] \tag{8}$$

In order to find β, the surface area of the sample is first measured, a small amount of fluid is adsorbed on the sample, the sample is reweighed to find C, a T_1 experiment is conducted and β is found using Equation 8. Usually, exponential relaxation is observed since a wide pore size range is

not filled and the determination of T_1 is straightforward. However, for materials with a complex structure such as coal, single exponential behavior is not observed, and Equation 8 must be modified by weighting with the T_1 distribution as described elsewhere [22]:

$$\beta = 2 / [SA\ C] \sum_{j=1}^{N} f(T_{1j})\ [1/T_{1j} - \alpha]\ \Delta T_{1j} \qquad (9)$$

The T_1 distribution function used in Equation 9 is that deconvoluted from the experimental magnetization data via NNLS. This approach for β determination has the advantage that it is conducted using the same sample as will be used for pore structure analysis. For a given fluid, temperature, and proton frequency, the β determination need not be carried out unless the sample surface chemistry is significantly different than materials analyzed previously since β does not appear to be a strong function of surface chemistry.

EXPERIMENTAL

Ten United States coals representing a range of rank and geographic origin were obtained from the Penn State coal bank (PSOC). These coals are summarized in Table 1. In addition to coal, a sample of Spheron-6 carbon black has been analyzed in order to provide a comparison of the NMR method with conventional pore structure analysis tools.

Sorption measurements of nitrogen at 77 K and carbon dioxide at 273 K were conducted using a Quantasorb flow-type surface area analyzer. Before analysis, samples (-325/+400 mesh) were outgassed in a dry helium stream at approximately 383 K. Outgassing was continued until a thermal conductivity

Table 1. Selected PSOC coals for pore structure analysis.

Coal	Location	Rank
PSOC-68	Lower Sunnyside, Emery Co., UT	HVBB
PSOC-88	Zap, Mercer Co., ND	Lignite A
PSOC-118	Tioga, Nicholas Co., WV	HVAB
PSOC-128	Lower Kittanning, Cambria Co., PA	LVB
PSOC-309	#8 seam, San Juan Co., NM	HVCB
PSOC-310	#7 seam, San Juan Co., NM	HVCB
PSOC-311	#6 seam, San Juan Co., NM	HVCB
PSOC-856	Juanita C, Gunnison Co., CO	HVBB
PSOC-869	Primrose, Schuykill, PA	AN
PSOC-1354	Illinois #6, Douglas Co., IL	HVCB

detector indicated that outgassing was complete. Outgassing typically took 3 to 8 hours. Carbon dioxide measurements were made at three relative pressure values between 0.0024 and 0.0167. With a flow-type adsorption analyzer, a temperature difference is used to desorb gas from the sample surface. For this study, the sample was heated to approximately 373 K to desorb gas after each adsorption point at 273 K. The surface area was calculated using the Dubinin-Radushkevich equation and a molecular cross-sectional area of 0.210 nm^2. For the nitrogen surface area, five relative pressure values in the range of 0.05 to 0.35 were used. Surface areas were calculated using the BET equation and a cross-sectional area of 0.162 nm^2. In addition, the pore volume with radius less than approximately 33 nm was obtained from nitrogen desorption at a relative pressure of 0.97.

Relaxation experiments were performed at 303 K using a Spin-Lock Ltd. CPS-2 pulse NMR with a 4.7 kGauss magnet. The corresponding proton Larmor frequency is 20 MHz. The inversion recovery or 180°-τ-90° method was used where a 180° pulse inverts the magnetization and after a time period, τ, a 90° pulse measures the degree of relaxation back to the equilibrium value, M_0. Durations of the 90° and 180° radiofrequency pulses were approximately 5 and 10 μs. The free induction decay (FID) was measured using a Nicolet 2090 digital oscilloscope interfaced to an IBM CS-9000 computer. The magnitude of τ was varied nonuniformly from 100 μs to 9 s. Typically, 40 to 50 different τ values were used to characterize the decay curve, $M(\tau)$. Before analysis, samples (-60/+140 mesh) were evacuated (≈10 μm Hg) in a sealed container and water was backfilled into the container. Water vapor and the coal sample were allowed to equilibrate at approximately 333 K for 12 to 24 hours. These conditions were found to be sufficient to completely saturate the sample. The water content was found gravimetrically by drying

the sample after NMR analysis. Another set of experiments were conducted by saturating the samples over a salt solution with 97% relative humidity at ambient temperature for 72 hours.

After the saturation step, a typical NMR experiment required approximately 15 minutes to perform. When plotted on semi-log axes, the experimental magnetization data was nonlinear, and hence the relaxation not singly exponential. T_1 distributions were obtained from the $M(\tau)$ data using both NNLS and regularization. For regularization, an optimum value of the regularization parameter, δ_{opt}, was not obtained for every sample as a result of the complex T_1 distributions associated with coal. Therefore, δ_{opt} was assumed constant at an average value of 0.006 for these calculations. For the Spheron-6 sample, a δ_{opt} value of 0.004 was obtained. In order to extract pore size distributions from the T_1 distributions, a pore shape assumption is required for pores in the size range of 0.5 to 5.0 nm. For coal, the pore shape was assumed to be slit-shaped and the thickness of the surface-affected phase, Δ, was taken to be 0.3 nm. As discussed by Gallegos and co-workers [16], the calculated pore size distributions are relatively insensitive to these assumptions.

RESULTS

The surface area results calculated from the carbon dioxide and nitrogen adsorption experiments are presented in Figure 1 for all 10 samples on a dry basis. The results are presented in order of increasing carbon content. As is commonly observed for coals, the surface areas determined via carbon dioxide adsorption are significantly greater than nitrogen surface areas. The ratio of CO_2 to N_2 areas can be interpreted as a qualitative measure of microporosity. Of particular note is the lack of dependence of surface area

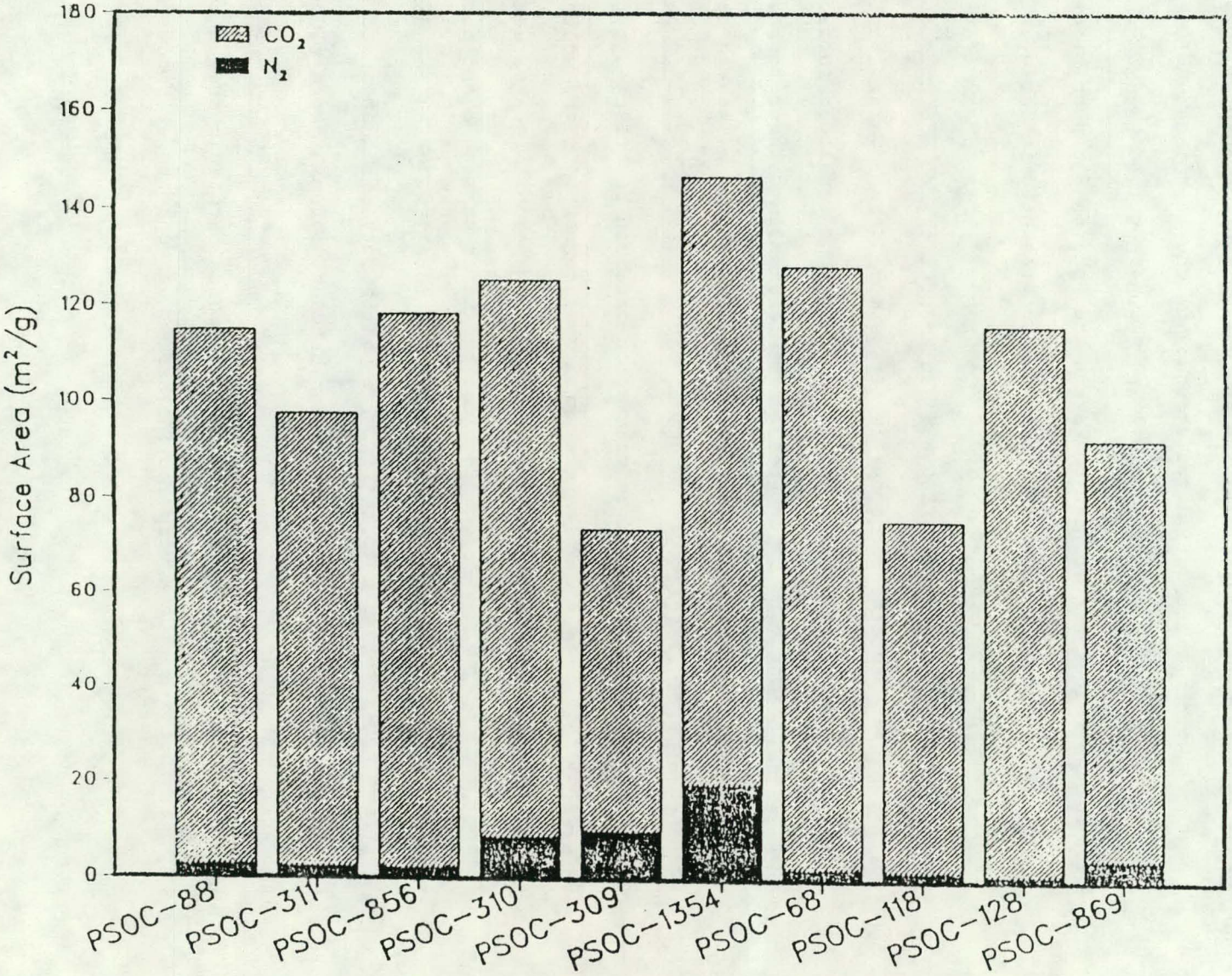

Figure 1. Coal surface areas via nitrogen and carbon dioxide adsorption.

on carbon content and the relative ratio of carbon dioxide to nitrogen surface area. Gan, Nandi and Walker [4] have previously reported a general trend of surface area (both CO_2 and N_2) with carbon content. They also note the relatively high N_2 surface areas observed for Illinois #6 coals (such as PSOC-1354 used in this study). For the Spheron-6 carbon black, surface areas determined from both nitrogen and carbon dioxide adsorption were identical within the experimental accuracy of the techniques ($\approx$103 m^2/g).

The technique described by Davis and co-workers [22] has been used to determine β values for all ten coals and the Spheron-6 carbon black. The β value, ash content, and hydrogen content are presented in Table 2 in order of increasing carbon content. The β value varies over the range of coals studied, from 36.5 nm/s for PSOC 869, an anthracite, to 986 nm/s for PSOC 88, a lignite. Neglecting the one lignite sample, the β variation is significantly reduced. This β variation may be the result of surface chemistry, paramagnetic impurities, cross-relaxation with protons in the solid matrix and experimental measurement variability. The ash content can be taken as a gross relative measure of paramagnetic material in each sample. Since the spin-lattice relaxation rate can be affected by paramagnetic impurities, this is a particular concern for the successful application of the NMR technique to coals. However, it is apparent from Table 2 that only a weak or no correlation exists between β and paramagnetic impurities, i.e. paramagnetic impurities are most likely not the dominating contributing factor to β variation. The possibility of an enhanced surface relaxation rate due to cross-relaxation between protons in the fluid and in the solid matrix has been suggested by Glaves and co-workers [23] as a reason for different β values. Weak correlation between hydrogen content and β is observed, but a very small hydrogen content range is covered and

Table 2 Values of β determined from Equation 8 and carbon dioxide surface areas.

COAL	% ASH-Dry	%H-Dry	β (nm/s)
PSOC-88	11.9	4.54	986
PSOC-311	17.6	4.81	139
PSOC-856	3.7	5.26	74.8
PSOC-310	8.8	5.20	209
PSOC-309	20.3	4.58	310
PSOC-1354	10.4	4.46	103
PSOC-68	5.1	5.44	73.9
PSOC-118	15.4	4.26	66.1
PSOC-128	13.6	4.08	213.7
PSOC-869	11.4	1.55	36.5
Spheron-6	-	-	32.7

significant experimental uncertainty exists in the β determination. This uncertainty arises from the determination of surface area, C, and T_1.

Pore size distributions for Spheron-6 have been determined via the conventional methods of mercury porosimetry and nitrogen condensation (desorption branch) for comparison to the spin-lattice relaxation method. The results of this comparison are presented in Figure 2. Agreement between the three methods is quite good. Both mercury porosimetry and nitrogen condensation predict a slightly smaller pore radius corresponding to the maximum in the pore volume distribution. However, the intrusion curve for porosimetry and the desorption branch for nitrogen are usually taken to be measures of the neck or constriction size in a pore. Therefore, one would expect the distribution of hydraulic radius to occur at slightly larger pore size, as is observed. Also, network/percolation effects will skew porosimetry and condensation results to smaller pore radius. We should note that only the total surface area has been used in the determination of β, and hence, the NMR pore size distribution is completely independent of both the porosimetry and condensation methods.

As discussed previously, samples were saturated at water relative pressures of both 0.97 and ≈1.0. For a relative pressure of 0.97, water will only condense in pores with radii less than approximately 30 nm. For ≈1.0, water will condense in most submicron pores, surface roughness/porosity and interparticle contacts. A comparison between the pore size distributions calculated for a single lignite coal, PSOC-88, is presented in Figure 3. As expected, the upper pore size limit for the 0.97 distribution is significantly less than for 1.0. Both distributions have a maximum in the PSD (pore size distribution) at approximately 5-10 nm. In addition, a second maximum at ≈200 nm is obtained when the sample is saturated at higher

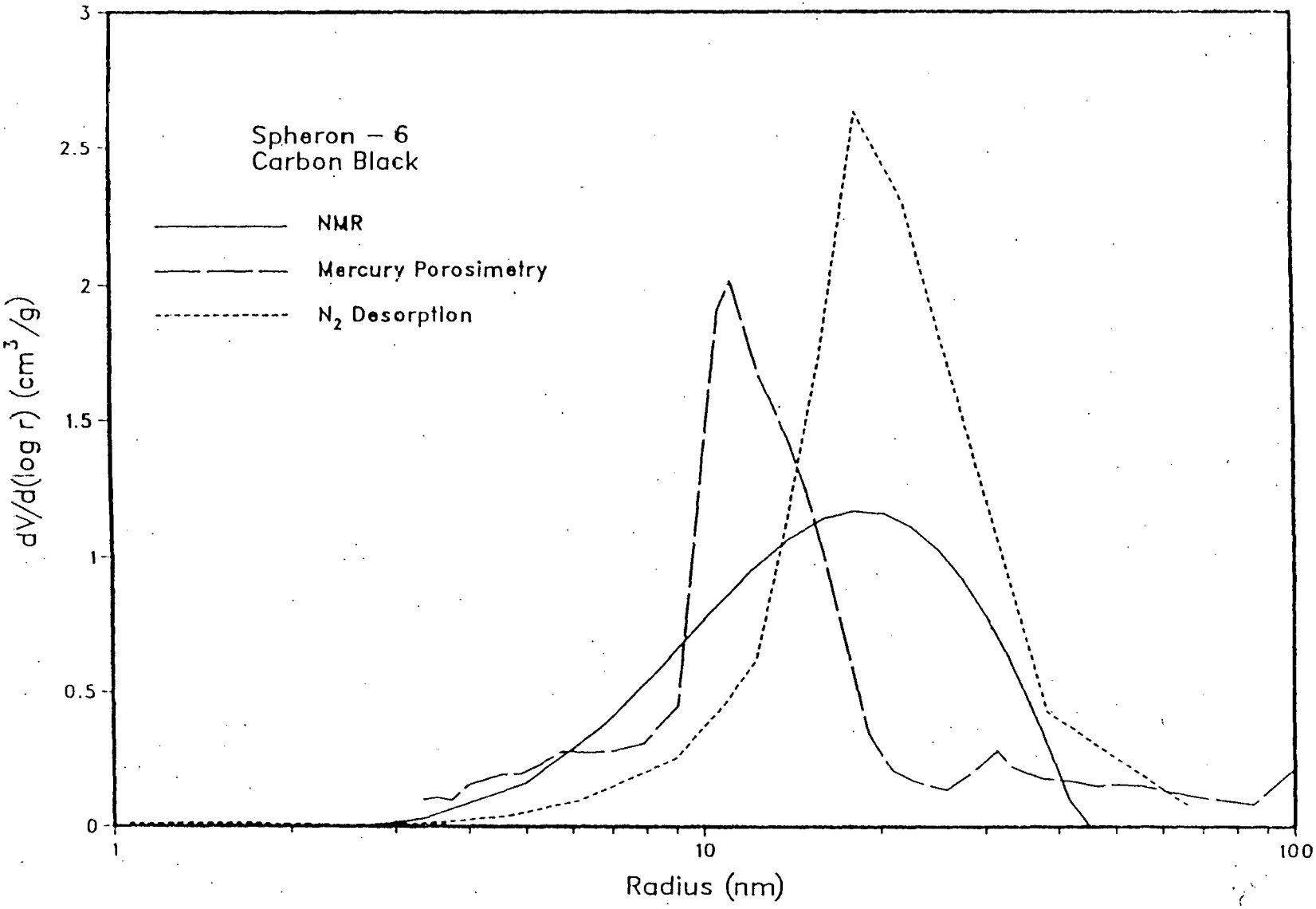

Figure 2. Spheron-6 pore size distribution via NMR, mercury porosimetry, and nitrogen adsorption/condensation.

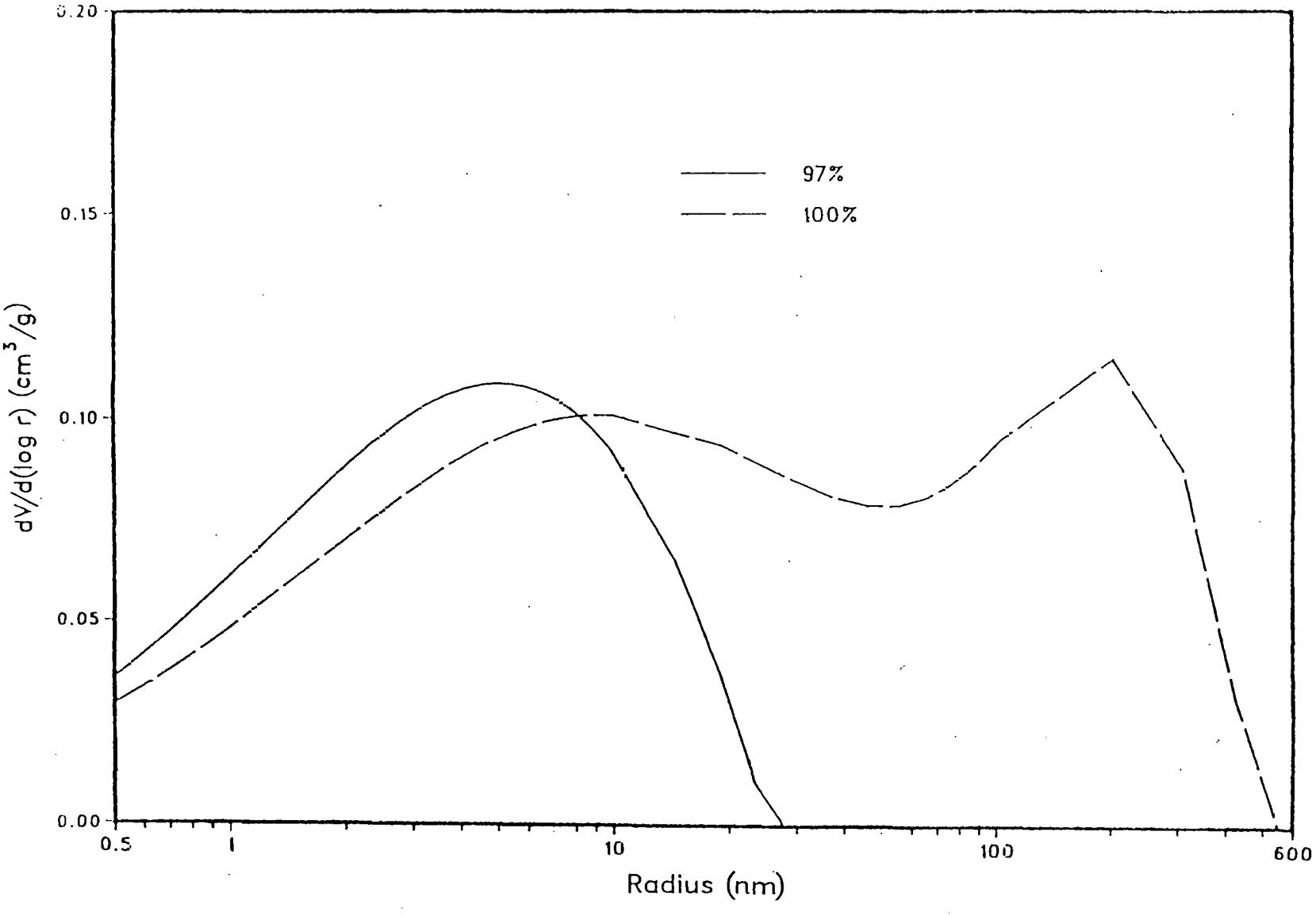

Figure 3. NMR pore size distribution for PSOC-88 saturated at different relative pressures.

relative pressure. As with the conventional pore analysis methods, the interpretation of pore size information in the larger pore sizes is complicated by surface roughness/porosity and interparticle void filling effects. The standard approach to this problem is to use a wide range of particle sizes. Both PSD's have a finite value at the lower pore size limit of 0.5 nm indicating the presence of pore volume with radius less than this limit. From the spin-lattice relaxation measurements, the fraction of pore volume in pores with size less than 0.5 nm may be obtained but the calculated distribution in this range has no physical meaning. Although a pore size distribution has been calculated for this lignite sample, a caution should be recalled concerning the use of this analysis model for low rank coals, this being due to the possible altering of pore structure upon sorption of the fluid.

Pore size distributions for three coals (PSOC-309, 310, 311) obtained from three different seams of the same Fruitland formation of the San Juan Basin of New Mexico are presented in Figure 4. All three samples were saturated at a relative pressure of ≈1.0. The reproducibility of the NMR method is demonstrated by the similar PSD's obtained for these three similar coals despite the variation in β for the coals. A bidisperse distribution is observed for all three samples with one maximum at the lower pore size limit and the second maximum near 50 nm. The NMR PSD's are consistent with the CO_2/N_2 surface area ratios, PSOC 311 showing the most microporosity and the highest ratio, while PSOC 309 shows the least microporosity and the lowest ratio.

Figure 5 includes NMR-derived PSD's for four different coals of similar rank. The PSOC-68, 118 and 856 all have similar high ratios of CO_2 to N_2 surface areas as compared to the PSOC-1354 sample but all have nitrogen pore

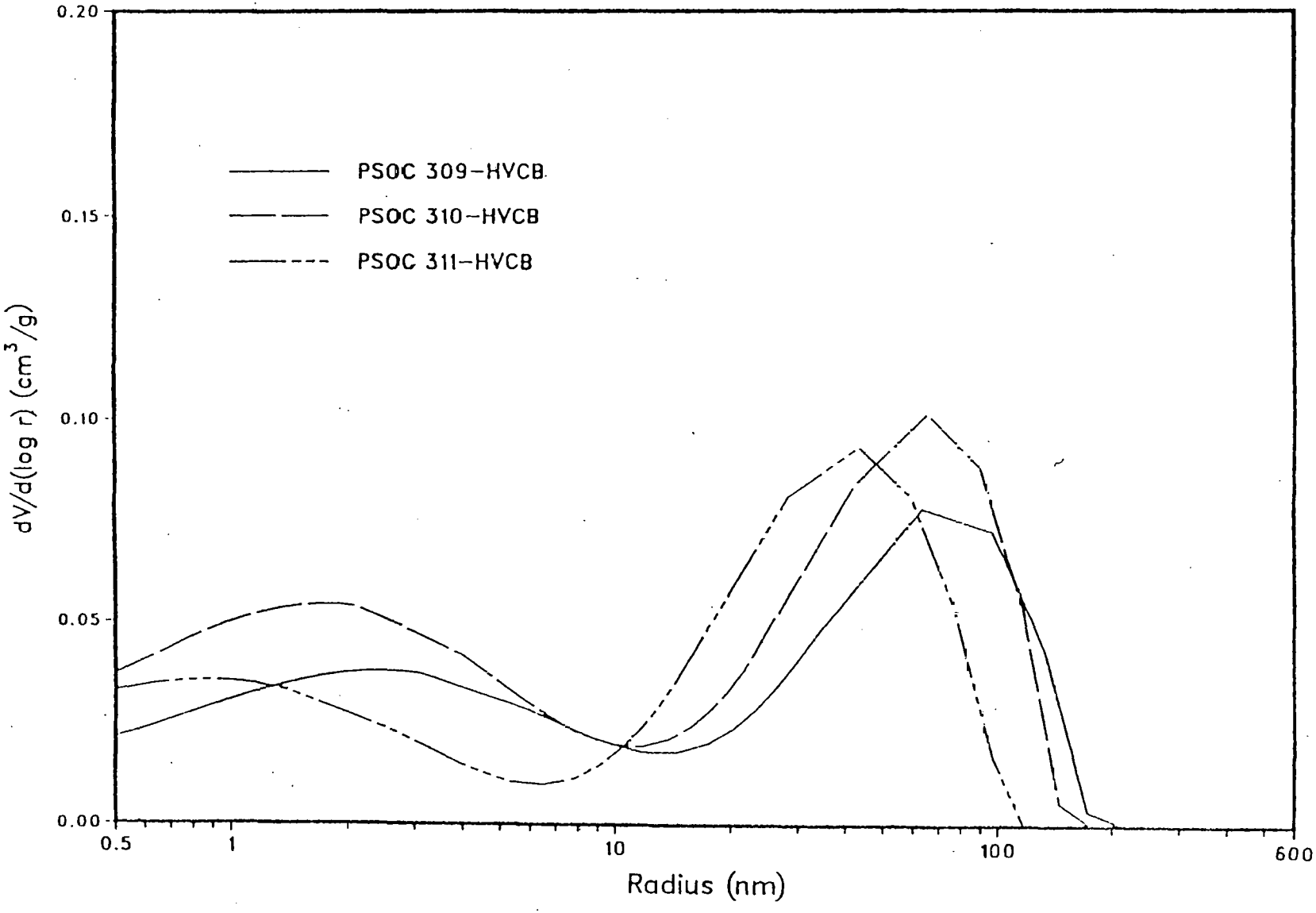

Figure 4. NMR pore size distributions for coals from the same formation.

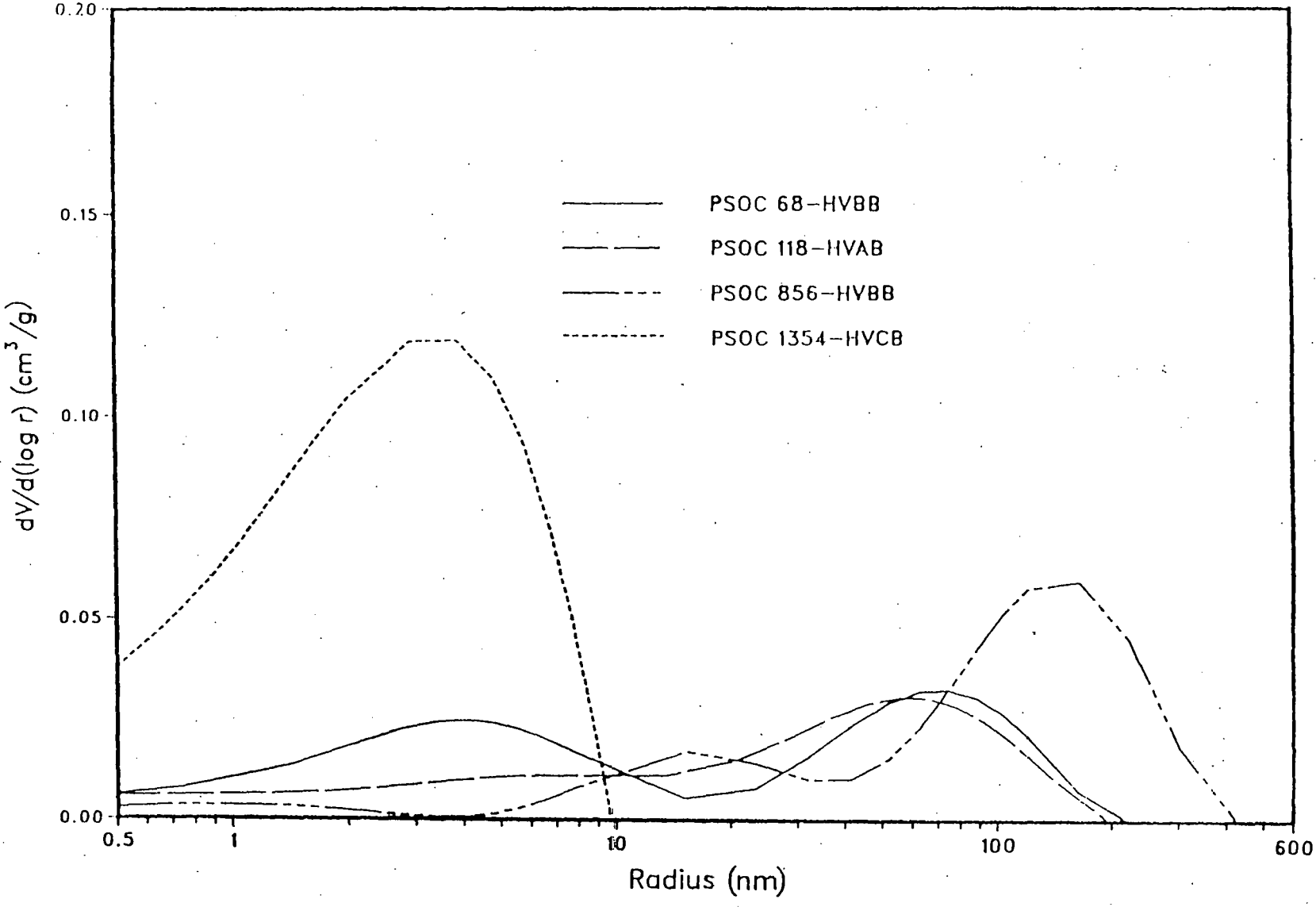

Figure 5. NMR pore size distributions for coals of similar rank.

volumes on the same order of magnitude. This indicates that of the total pore volume which is accessable to nitrogen, the average pore size for the 1354 sample is much lower than the three other coals. For mercury porosimetry of the PSOC-1354 sample, a large quantity of pore intrusion/collapse was noted at high pressures (>10,000 psia) as compared to the other coals in this set [8]. This is consistent with the NMR results (i.e., the large maximum for PSOC-1354 in the vicinity of 4 nm).

Pore size distributions for three coals of varying rank are presented in Figure 6. As expected, the lignite sample has a wide distribution with maximum pore size on the order of 500 nm. In general, as rank increases, the width of the pore size distribution decreases. The fact that the anthracite appears to have a larger pore size range than the low volatile bituminous PSOC-128 sample is somewhat of a surprise. However, this finding is supported by a review of our surface area results. PSOC-128 has a much higher ratio of carbon dioxide surface area to nitrogen surface area indicating the presence of a substantial quantity of microporosity.

In addition to pore size distribution information for pore sizes greater than 0.5 nm in radius, the fraction of total pore volume contained in pores with size less than this lower cut-off may be obtained from spin-lattice relaxation measurements. This fraction is reported for each coal sample (saturated at 0.97 and ≈1.0) in Table 3. As would be expected, coals saturated at ≈1.0 have a lower fraction of volume in this size range than the 0.97 saturated samples. When fluid is added to larger pores, the relative fraction in the micropores will decrease. All coals exhibit significant fractions of pore volume in the microporous size range. This is one of the reasons for the large difference between the nitrogen and carbon dioxide surface areas.

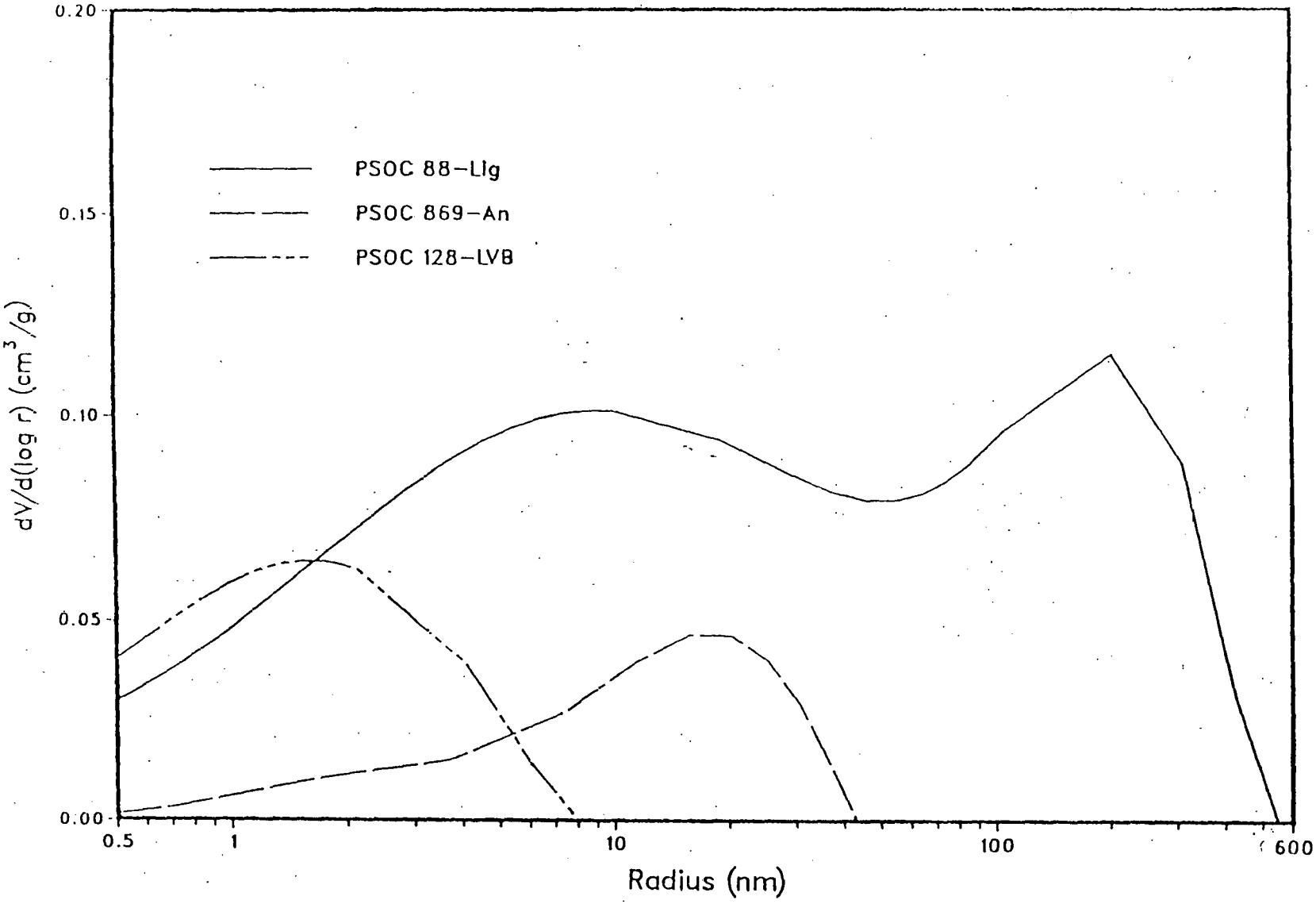

Figure 6. NMR pore size distributions for coals of varying rank.

Table 3 Fraction of total measured pore volume in pores with radius smaller than 0.5 nm.

COAL	$P/P_o = 0.97$	$P/P_o \approx 1.0$
PSOC-88	0.39	0.05
PSOC-311	0.25	0.18
PSOC-856	0.24	0.02
PSOC 310	0.16	0.16
PSOC-309	0.14	0.11
PSOC 1354	0.28	0.16
PSOC-68	0.19	0.10
PSOC-118	0.20	0.12
PSOC-128	0.18	0.26
PSOC-869	0.26	0.01

DISCUSSION

The comparison of pore size distributions obtained from spin-lattice relaxation measurements with conventional methods such as mercury porosimetry and/or nitrogen adsorption/condensation is difficult/impossible for coals. However, for materials such as carbon black, comparison between the methods may be made and agreement is excellent when one correctly interprets the information obtained from porosimetry/condensation. For coal, only qualitative comparisons of NMR pore structure information with nitrogen/carbon dioxide surface areas may be made. Based upon the comparisons that can be made between spin-lattice measurements and conventional approaches, it appears that this new approach results in reasonable and useful pore structure information which is not available via other methods.

ACKNOWLEDGEMENTS

This work has been funded by the US Department of Energy's Pittsburgh Energy Technology Center (DE-FG22-85PC80519). Adsorption and mercury intrusion measurements were performed by N. Olague, J. Pena and D. Stermer. The authors would like to thank L. Brown and J. Brown of the Los Alamos National Laboratory for arranging the loan of the 20 MHz NMR.

NOMENCLATURE

f_b - Fraction of fluid in the bulk phase.
f_s - Fraction of fluid in the surface phase.
$f(T_1)$ - Distribution of pore volume with T_1.
$M(\tau)$ - Magnetization at time τ.
M_0 - Equilibrium magnetization.
PV - Specific pore volume.

r_p = Hydraulic radius, 2PV/SA.

SA = Specific surface area.

T_1 = Observed spin-lattice relaxation time.

T_{1b} = Bulk spin-lattice relaxation time.

$T_{1surface}$ = Spin-lattice relaxation time of the surface-affected phase.

T_{1s} = $T_{1surface}$ divided by the surface phase thickness.

α = $1/T_{1b}$.

β = $2/T_{1s}$.

δ = Regularization smoothing parameter.

Δ = Thickness of the surface-affected phase.

τ = Delay time between 180° and 90° pulses.

REFERENCES

1. Anderson, R.B., Bayer, J., and Hofer, L.J.E., **Fuel**, 44, 443, (1965).

2. Marsh, H., and Siemieniewska, T., **Fuel**, 44, 355, (1965).

3. Zwietering, P. and van Krevelen, D.W., **Fuel**, 33, 331, (1954).

4. Gan, H., Nandi, S.P., and Walker, P.L., **Fuel**, 51, 272, (1972).

5. Toda, Y. and Toyoda, S., **Fuel**, 51, 199, (1972).

6. Debelak, K.A., and Schrodt, J.T., **Fuel**, 58, 732, (1979).

7. Spitzer, Z., **Powder Tech.**, 29, 177, (1981).

8. Gallegos, D.P., Smith, D.M. and Stermer, D.L., STUDIES IN SURFACE SCIENCE AND CATALYSIS, G. Kreysa and A. Kral, Editors, Elsevier Press, Amsterdam, in press.

9. Lynch, L.J., and Webster, D.S., **Fuel**, 58, 429, (1979).

10. Lynch, L.J., and Webster, D.S., **J.Magn.Reson.**, 40, 259, (1980).

11. Cutmore, N.G., Sowerby, B.D., Lynch, L.J. and Webster, D.S., **Fuel**, 65, 34, (1986).

12. Lynch, L.J., Sakurovs, R., and Barton, W.A., **Fuel**, 65, 1108, (1986).

13. Brownstein, K.R. and Tarr, C.E., **J.Magn.Reson.**, 26, 17, (1977).

14. Woessner, D.E., **J.Magn.Reson.**, 39, 297, (1980).

15. Almagor, E., and Belfort, G., J.Colloid Interface Sci., 66, 146, (1978).

16. Gallegos, D.P., Smith, D.M., and Brinker, C.J., J.Colloid Interface Sci., in press.

17. Munn, K. and Smith, D.M., J.Colloid Interface Sci., 119, 117, (1987).

18. Brown, J.A., Brown, L.F., Jackson, J.A., Milewski, J.V., and Travis, B.J., Proc. of the SPE/DOE Unconventional Gas Recovery Symp., 201, (1981).

19. Gallegos, D.P. and Smith, D.M., J. Colloid Interface Sci., in press.

20. Butler, J.P., Reeds, J.A., and Dawson, S.V., SIAM J.Numer.Anal., 18, 381, (1981).

21. Gallegos, D.P., Munn, K., Stermer, D.L., and Smith, D.M., J.Colloid Interface Sci., 119, 127, (1987).

22. Davis, P.J., Gallegos, D.P., and Smith, D.M., Powder Tech., 53, 39, (1987).

23. Glaves, C.L., Davis, P.J., and Smith, D.M., Powder Tech., in press.

3 DISSEMINATION OF RESEARCH

3.1 REFEREED PUBLICATIONS

1) Gallegos, D.P., Munn, K., Smith, D.M. and Stermer, D.L., " A NMR Technique for the Analysis of Pore Structure: Application to Well-Characterized Porous Solids," **Journal of Colloid and Interface Science**, 119, 127-139, (1987).

2) Gallegos, D.P., and Smith, D.M., "A NMR Technique for the Analysis of Pore Structure: Determination of Continuous Pore Size Distributions," **Journal of Colloid and Interface Science**, 122:1, 143-153, (1988).

3) Smith, D.M., and Gallegos, D.P., "Analysis of Pore Structure via Spin-Lattice Relaxation Measurements," CHARACTERIZATION OF POROUS SOLIDS, K.K. Unger, J. Rouquerol, K.S.W. Sing, H. Kral, Editors, Elsevier Press, Amsterdam, 391-400, (1988).

4) Gallegos, D.P., Stermer, D.L. and Smith, D.M., "Pore Structure Analysis of American Coals," CHARACTERIZATION OF POROUS SOLIDS, K.K. Unger, J. Rouquerol, K.S.W. Sing, H. Kral, Editors, Elseview Press, Amsterdam, 509-518, (1988).

5) Glaves, C.L., Davis, P.J., Gallegos, D.P., and Smith, D.M., "Pore Structure Analysis of Coals via Low Field Spin-Lattice Relaxation Measurements," **ENERGY & FUELS**, 2, 662-8, (1988).

6) Olague, N.E., and Smith, D.M., "Gas Diffusion Measurements in American Coals," transmitted to **FUEL**, December, 1988.

3.2 PROCEEDINGS, PRESENTED PAPERS

1) Gallegos, D.P., Stermer, D.L., and Smith, D.M., "Pore Structure Analysis using NMR Relaxation, Mercury Porosimetry and Nitrogen Adsorption," Presented at the National Meeting of the Fine Particle Society, San Francisco, CA, July, 1986.

2) Stermer, D.L., Olague, N.E., Smith, D.M. and Williams, F.L., "Pore Structure Analysis of Coal," Presented at the National Meeting of the Fine Particle Society, San Francisco, CA, July, 1986.

3) Gallegos, D.P., Smith, D.M., Stermer, D.L., and Williams, F.L., "Application of Various Techniques to the Pore Structure Analysis of Coal," presented at the 11th Symposium of the Rocky Mountain Fuel Society, Salt Lake City, UT, (1987).

4) Smith, D.M., Davis, P.J., and Gallegos, D.P., "A Comparison of Surface Area Determination via Nitrogen Adsorption and NMR," presented at the 18th Annual Meeting of the Fine Particle Society, Boston, MA, 1987.

3.3 GRADUATE STUDENT THESIS

Kevin Munn (MS/UNM). "Characterization of Porous Media using NMR Spectroscopy." 5/85-5/86.

David Gallegos (MS/UNM) "NMR Analysis of Pore Structure." 5/86-7/87.

Chris Glaves (MS/UNM) "Static and Dynamic Pore Structure via Nuclear Magnetic Resonance." 9/86-5/88.

Natalie Olague (MS/UNM) "Packed Bed Studies of Diffusion in Porous Media." 5/86-6/88.